Understanding Quark Mass and Interquark Force

Review: arXiv:1411.7853 [hep-ph]

Y. Sumino

(Tohoku Univ.)

☆ Plan of Talk

1. Before 1998: Theoretical problem IR renomalon
2. Around 1998: Drastic improvement

   Discovery of renormalon cancellation, Interpretation
3. OPE of QCD potential with subtraction of renormalons

   Determination of α_s by matching OPE and lattice computation
4. Summary & Conclusions

Status of Static Potential

3-loop pert. QCD (fixed-order) vs. lattice comp.

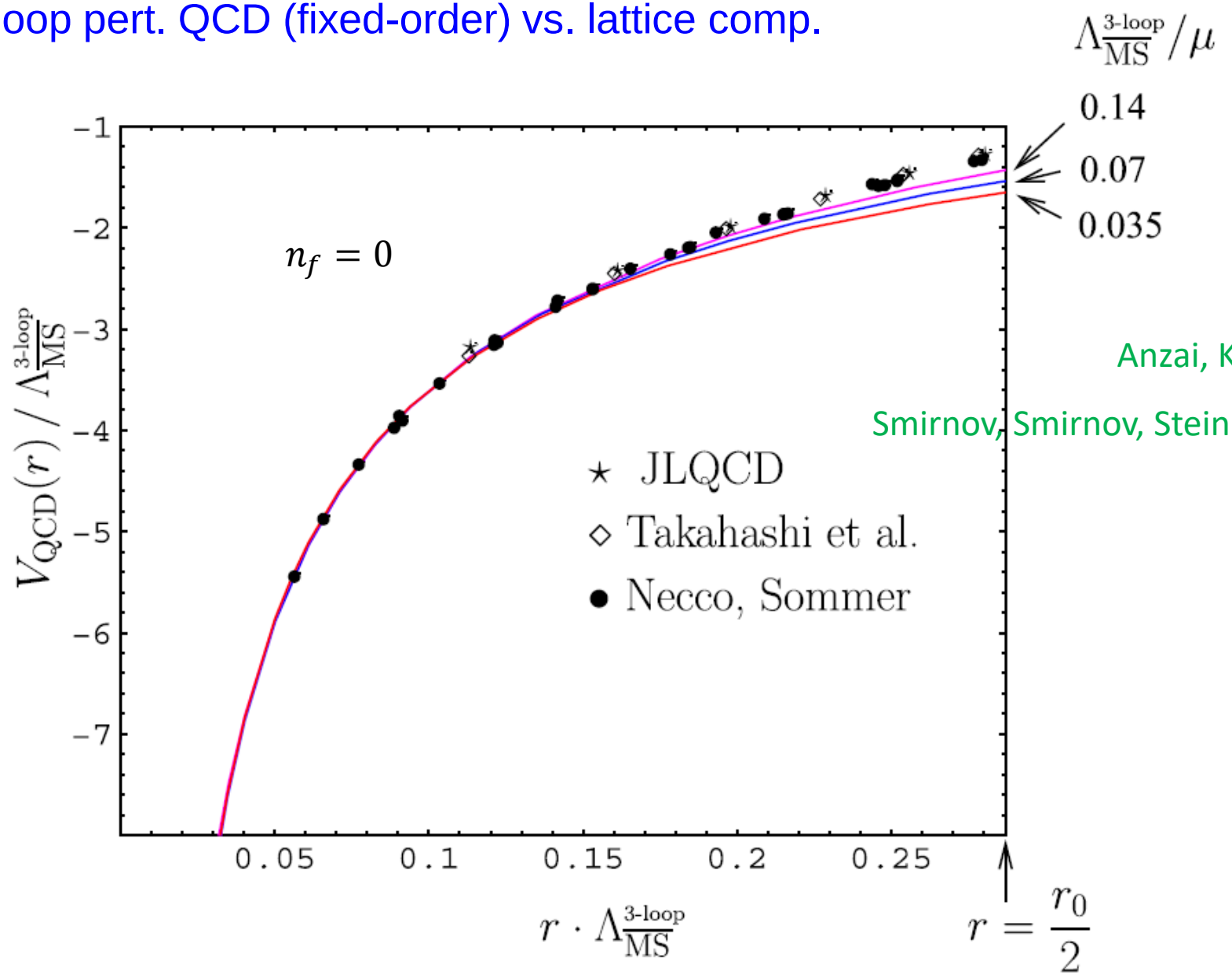

Anzai, Kiyo, YS

Smirnov, Smirnov, Steinhauser

Computation of spectrum of Positronium (e^+e^- boundstate)

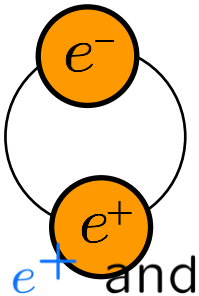

Free e^+ and e^-:

$$E_{\text{tot}} = 2m_{\text{pole}} - E_{\text{bin}}$$

Theoretical Framework (pNRQCD)

Brambilla, Pineda, Soto, Vairo

Compute quark-antiquark scattering amplitude in ordinary perturbative QCD.
$\Longrightarrow$ Determine a quantum-mechanical Hamiltonian in expansion in $1/c$:

$$\hat{H} = \hat{H}_0 + \frac{1}{c}\hat{H}_1 + \frac{1}{c^2}\hat{H}_2 + \cdots .$$

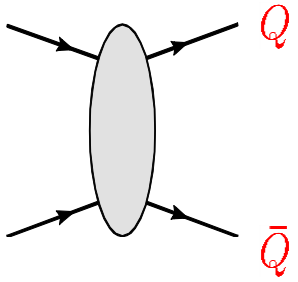

matching between pert. QCD and pNRQCD

$\Longrightarrow$ Solve the non-relativistic Schrödinger equation

$$\hat{H}\,\psi_X(r) = E_X\,\psi_X(r)$$

order by order in $1/c$ expansion. $\quad \dfrac{v}{c}, \quad \alpha_s = \dfrac{g_s^2}{\hbar c}$

Titard, Yndurain; Pineda, Yndurain

Kniehl, Penin, Smirnov, Steinhauser

$$\hat{H}_0 = \frac{\vec{p}^{\,2}}{m} - C_F \frac{\alpha_S}{r},$$

$$\hat{H}_1 = - C_F \frac{\alpha_S}{r} \cdot \left(\frac{\alpha_S}{4\pi}\right) \cdot \left\{\beta_0 \log(\mu'^2 r^2) + a_1\right\},$$

$$\hat{H}_2 = -\frac{\vec{p}^{\,4}}{4m^3} - C_F \frac{\alpha_S}{r} \cdot \left(\frac{\alpha_S}{4\pi}\right)^2 \cdot \left\{\beta_0^2 [\log^2(\mu'^2 r^2) + \frac{\pi^2}{3}] + (\beta_1 + 2\beta_0 a_1) \log(\mu'^2 r^2) + a_2\right\}$$
$$+\frac{\pi C_F \alpha_S}{m^2} \delta^3(\vec{r}) + \frac{3 C_F \alpha_S}{2m^2 r^3} \vec{L} \cdot \vec{S} - \frac{C_F \alpha_S}{2m^2 r}\left(\vec{p}^{\,2} + \frac{1}{r^2} r_i r_j p_j p_i\right) - \frac{C_A C_F \alpha_S^2}{2mr^2}$$
$$-\frac{C_F \alpha_S}{2m^2}\left\{\frac{S^2}{r^3} - 3\frac{(\vec{S}\cdot\vec{r})^2}{r^5} - \frac{4\pi}{3}(2S^2 - 3)\delta^3(\vec{r})\right\},$$

- $\Upsilon(1S)$: $M_{\Upsilon(1S)} = 9.94 - 0.10 - 0.15 - 0.20 - 0.26$ GeV

Kiyo, Mishima, YS

- $\Upsilon(2S)$: $M_{\Upsilon(2S)} = 9.94 - 0.06 - 0.11 - 0.22 - 0.41$ GeV

$\mathcal{O}(\alpha_s^0)$ $\mathcal{O}(\alpha_s^2)$ $\mathcal{O}(\alpha_s^3)$ $\mathcal{O}(\alpha_s^4)$ $\mathcal{O}(\alpha_s^5)$

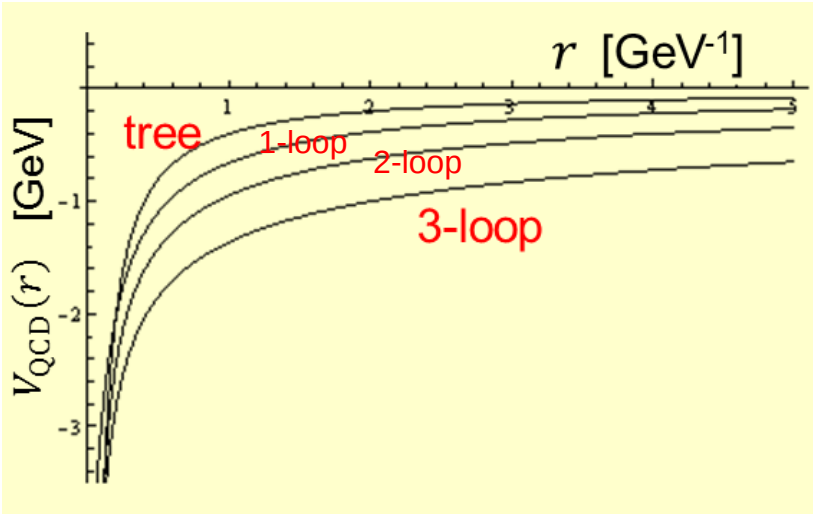
r [GeV-1]
tree
1-loop
2-loop
3-loop
$V_{QCD}(r)$ [GeV]

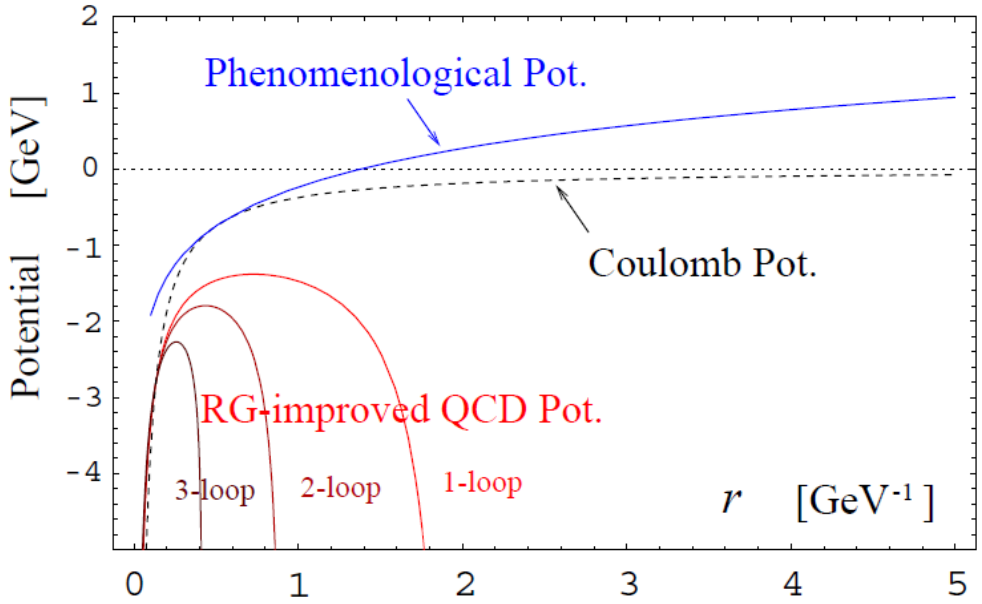
Phenomenological Pot.
Coulomb Pot.
RG-improved QCD Pot.
3-loop
2-loop
1-loop
Potential [GeV]
r [GeV-1]

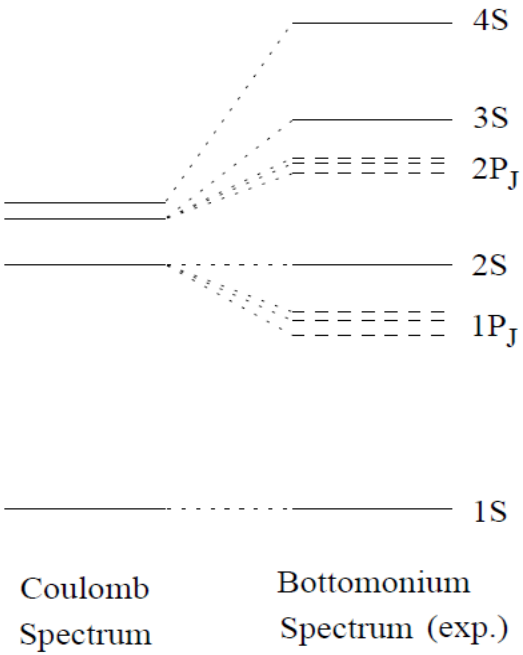
4S
3S
2P$_J$
2S
1P$_J$
1S
Coulomb Spectrum
Bottomonium Spectrum (exp.)

Accuracy of perturbative predictions for QCD potential improved drastically around year 1998.

Pineda
Hoang,Smith,Stelzer,Willenbrock
Beneke

If we re-express the quark pole mass ($m_{\rm pole}$) by the $\overline{\rm MS}$ mass ($m_{\overline{\rm MS}}$), IR renormalons cancel in $E_{\rm tot}(r) = 2m_{\rm pole} + V_{\rm QCD}(r)$.

$$V_{\rm LL}(r) = -\int \frac{d^3\vec{q}}{(2\pi)^3} e^{i\vec{q}\cdot\vec{r}} C_F \frac{4\pi\alpha_{\rm 1L}(q)}{q^2}$$

$$m_{\rm pole} \simeq m_{\overline{\rm MS}}(\mu) + \frac{1}{2}\int_{q<\mu} \frac{d^3\vec{q}}{(2\pi)^3} C_F \frac{4\pi\alpha_{\rm 1L}(q)}{q^2}$$

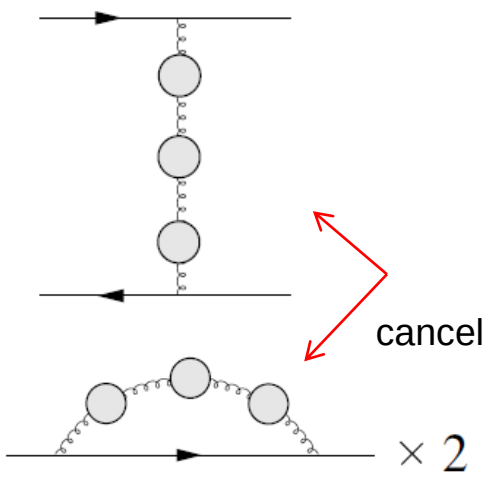

Expanding $e^{i\vec{q}\cdot\vec{r}} = \underline{1} + i\vec{q}\cdot\vec{r} + \frac{1}{2}(i\vec{q}\cdot\vec{r})^2 + \cdots$ for small q, the leading renormalons cancel . ⇨ much more convergent series

Residual renormalon: $\Lambda \times \left\langle (\vec{q}\cdot\vec{r})^2 \right\rangle \sim \Lambda \times \left(\Lambda\, r\right)^2 \ll \Lambda$

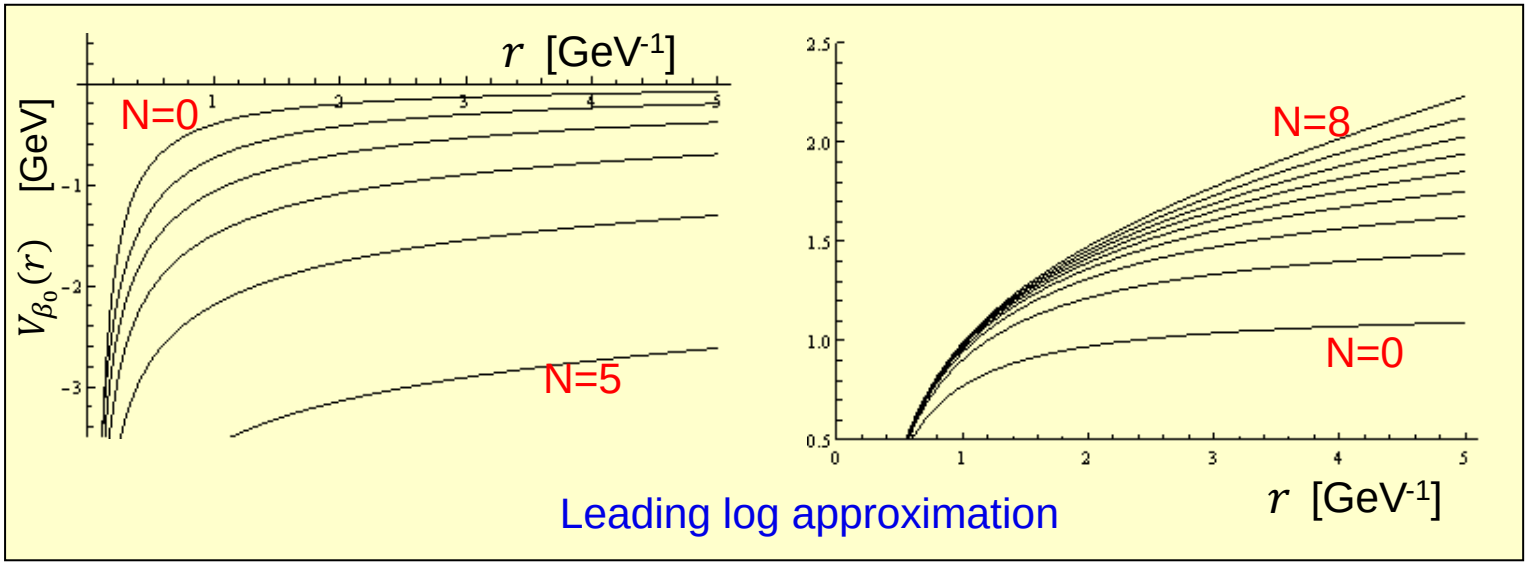

Leading log approximation

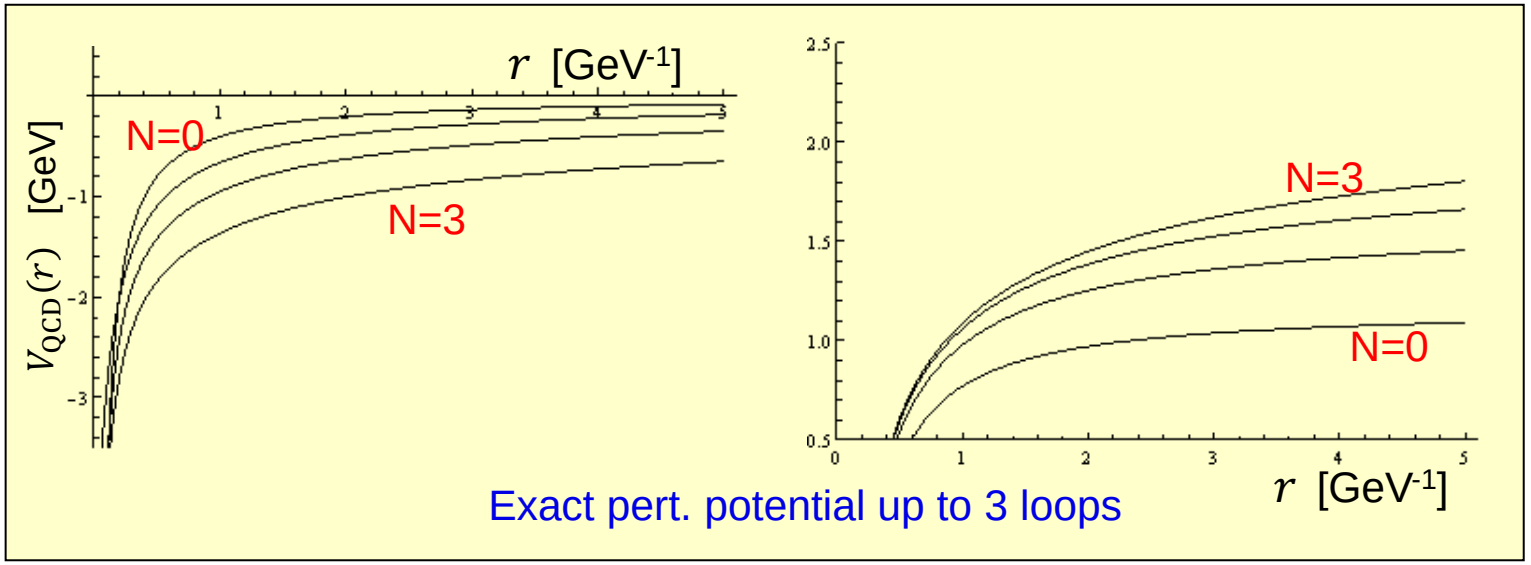

Exact pert. potential up to 3 loops

μ dependence and convergence of $M_{Q\bar{Q}}(1S)$

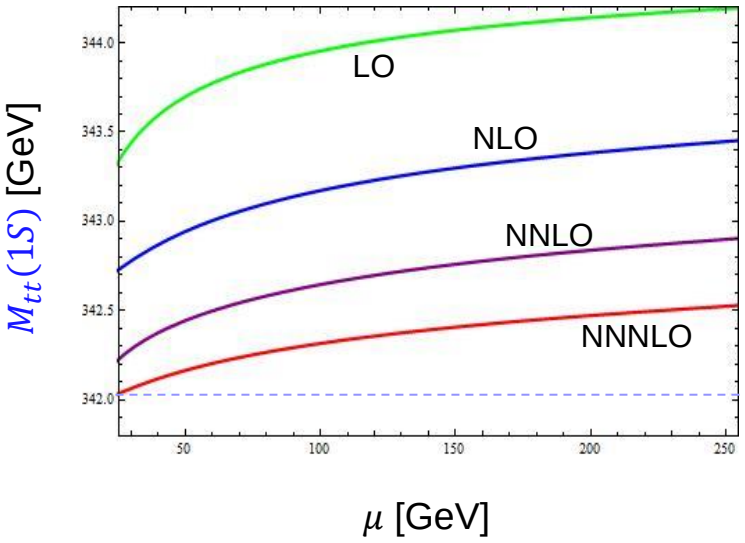

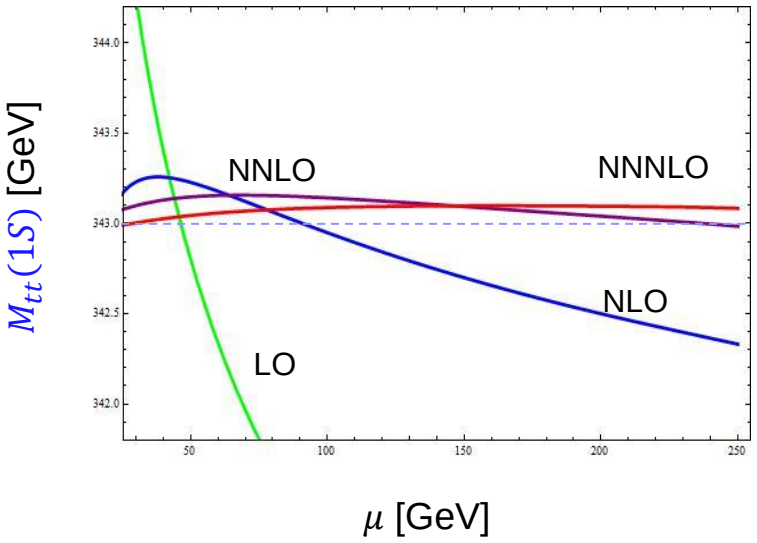

- $\Upsilon(1S)$: $M_{\Upsilon(1S)} = 9.94 - 0.10 - 0.15 - 0.20 - 0.26$ GeV (Pole-mass scheme)
  $= 8.43 + 0.72 + 0.25 + 0.07 - 0.02$ GeV ($\overline{\text{MS}}$ scheme)
- $\Upsilon(2S)$: $M_{\Upsilon(2S)} = 9.94 - 0.06 - 0.11 - 0.22 - 0.41$ GeV (Pole-mass scheme)
  $= 8.43 + 1.17 + 0.26 + 0.10 - 0.04$ GeV ($\overline{\text{MS}}$ scheme)

μ dependence and convergence of $M_{Q\bar{Q}}(1S)$

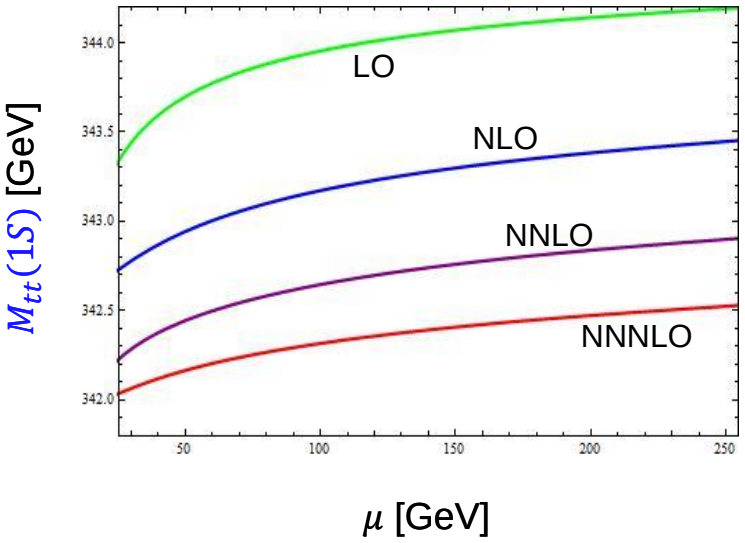

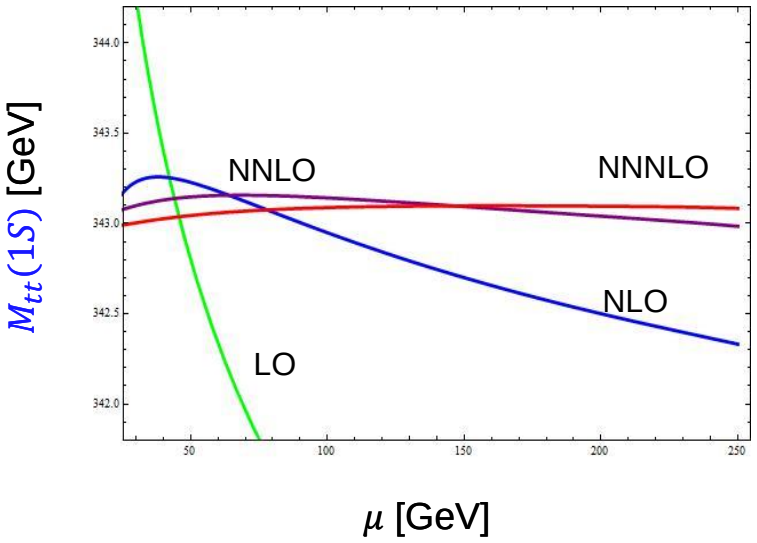

General feature of QCD beyond large b_0 or leading-log approx.

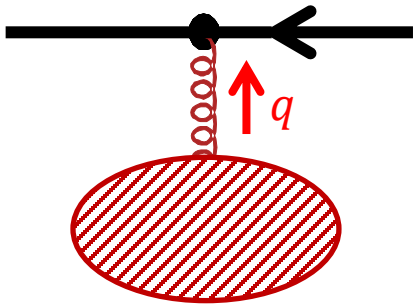

$A_\mu(q)\, j^\mu(-q)$

$j^\mu(x) = \delta^{\mu 0}\delta^3(\vec{x} - \vec{r}/2)$

Couples to total charge as $q \to 0$.

μ dependence and convergence of $M_{Q\bar{Q}}(1S)$

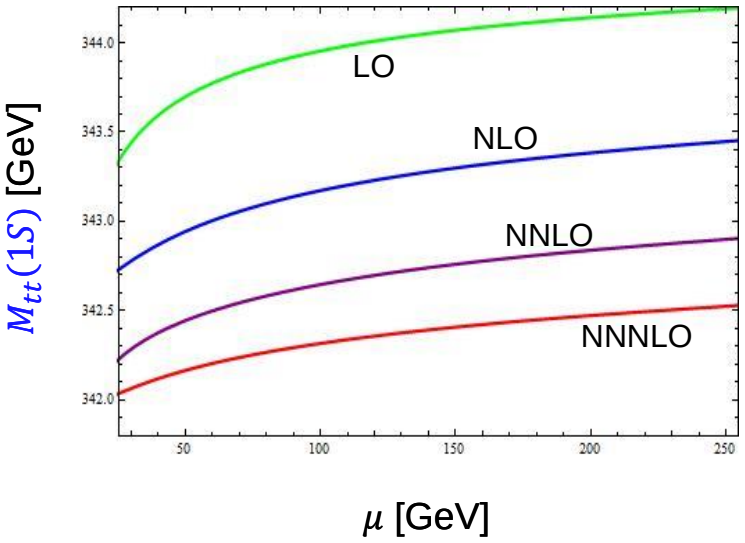

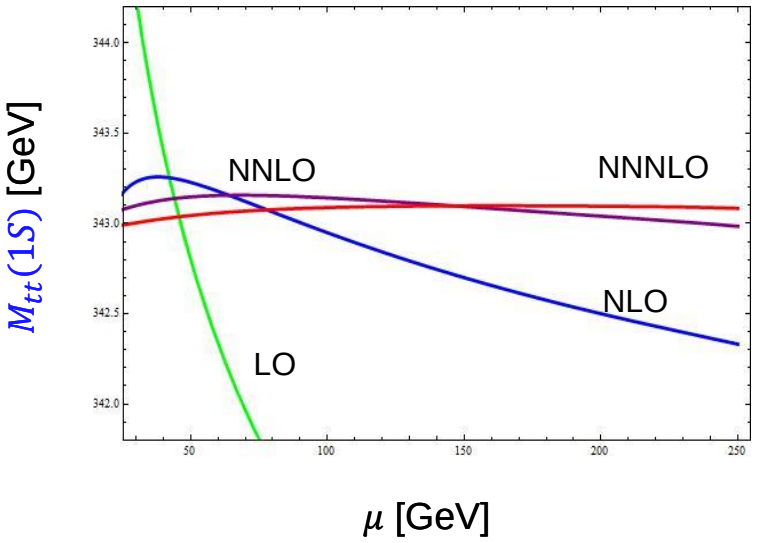

General feature of QCD beyond large b_0 or leading-log approx.

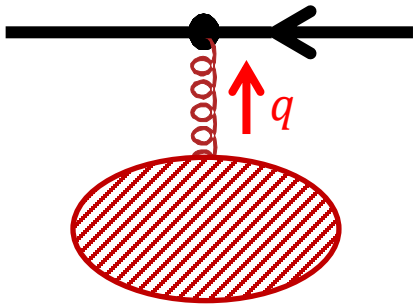

$A_\mu(q)\, j^\mu(-q)$

$j^\mu(x) = \delta^{\mu 0}\delta^3(\vec{x} - \vec{r}/2)$

Couples to total charge as $q \to 0$.

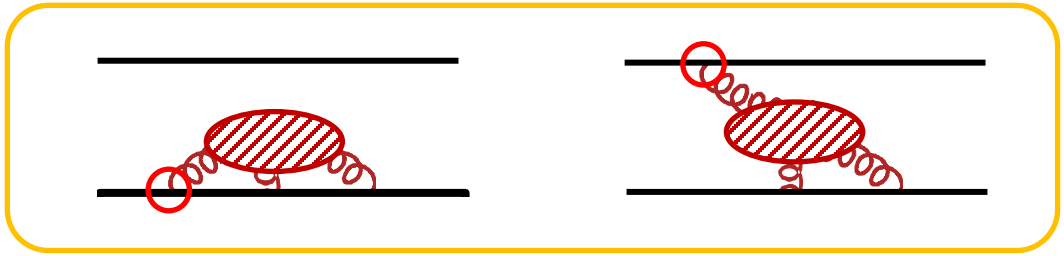

Pole mass m_{pole}

$0 < \lambda_g < \infty$

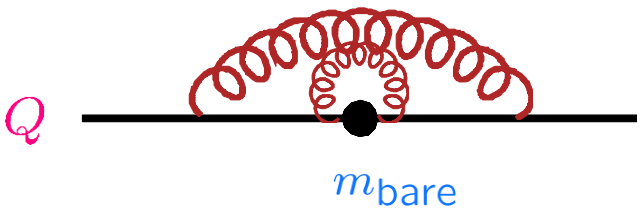

$\overline{\text{MS}}$ mass $\overline{m} \equiv m_{\overline{\text{MS}}}(m_{\overline{\text{MS}}})$

$0 < \lambda_g < 1/\overline{m}$

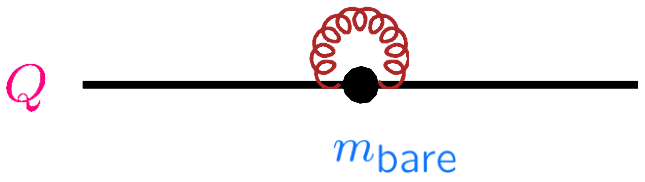

Computation of spectrum of Heavy Quarkonium ($Q\bar{Q}$ boundstate)

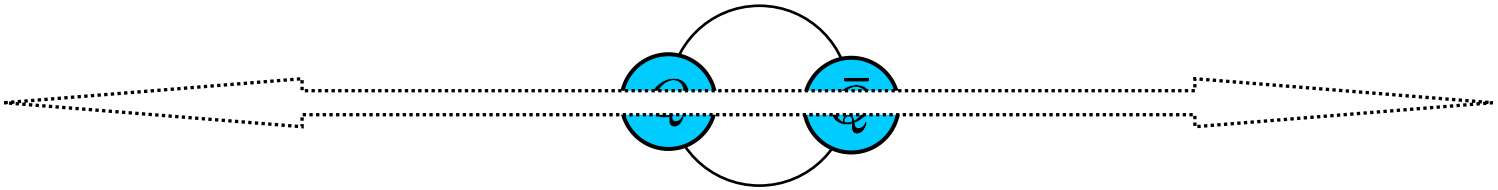

Free Q and $\bar{Q}$: $E_{\text{tot}} = 2m_{\text{pole}} - E_{\text{bin}}$ } not well-defined

Poorly convergent perturbative series

Pole mass m_{pole}

$0 < \lambda_g < \infty$

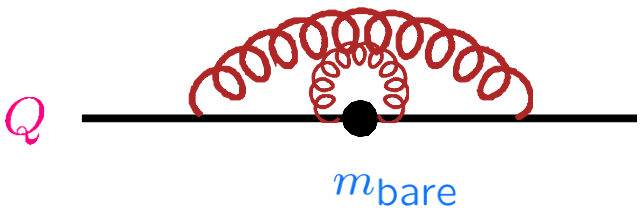

$\overline{\text{MS}}$ mass $\overline{m} \equiv m_{\overline{\text{MS}}}(m_{\overline{\text{MS}}})$

$0 < \lambda_g < 1/\overline{m}$

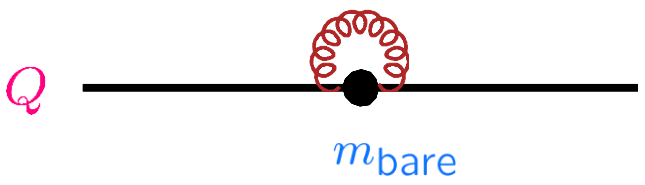

Computation of spectrum of Heavy Quarkonium ($Q\bar{Q}$ boundstate)

Using $\overline{\text{MS}}$ mass $\quad 2m_{\text{pole}} = 2\overline{m}\,(1 + c_1\,\alpha_S + c_2\,\alpha_S^2 + c_3\,\alpha_S^3 + \cdots)$

$E_{\text{tot}} =$ 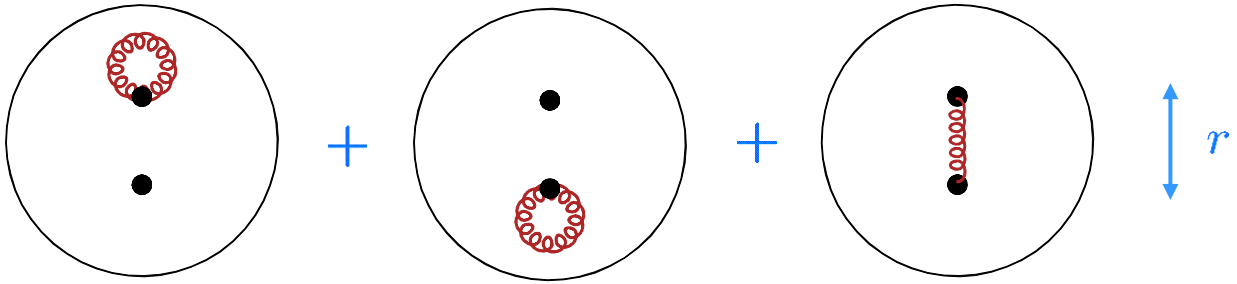 $+$ $+$

IR gluons $\lambda_g \gg r$ decouple ➡ much more convergent series

Rapid growth of masses of excited states originates from rapid growth of self-energies of Q & $\overline{Q}$ due to IR gluons.

Brambilla, Y.S., Vairo

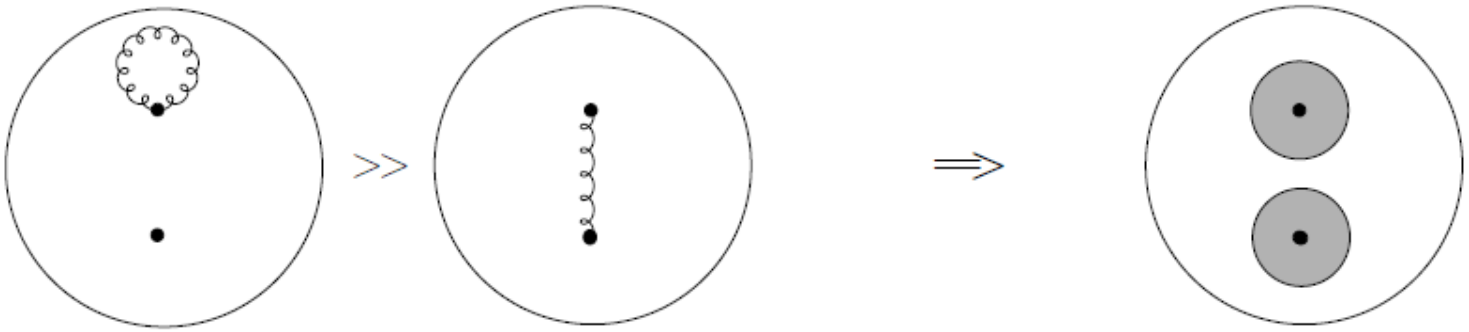

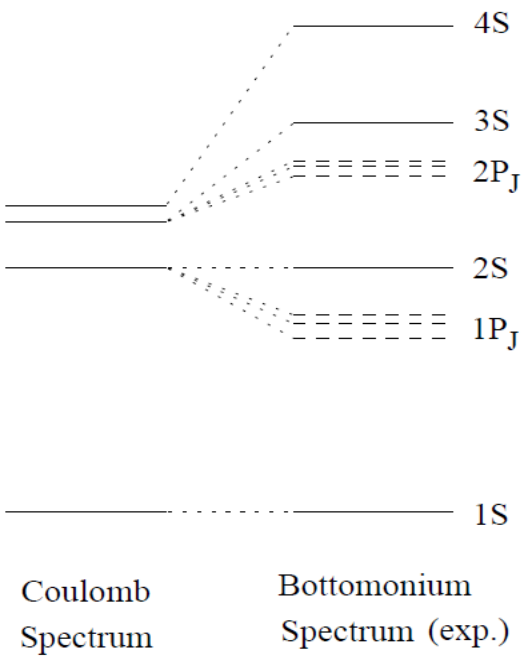

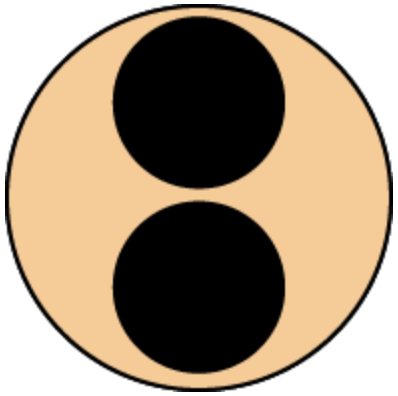

$$E_X \approx 2m_b^{\overline{MS}}(\mu) + \int_0^{\mu} dq\, f_X(q)\alpha_s(q)$$

Brambilla,YS,Vairo
Recksiegel,YS

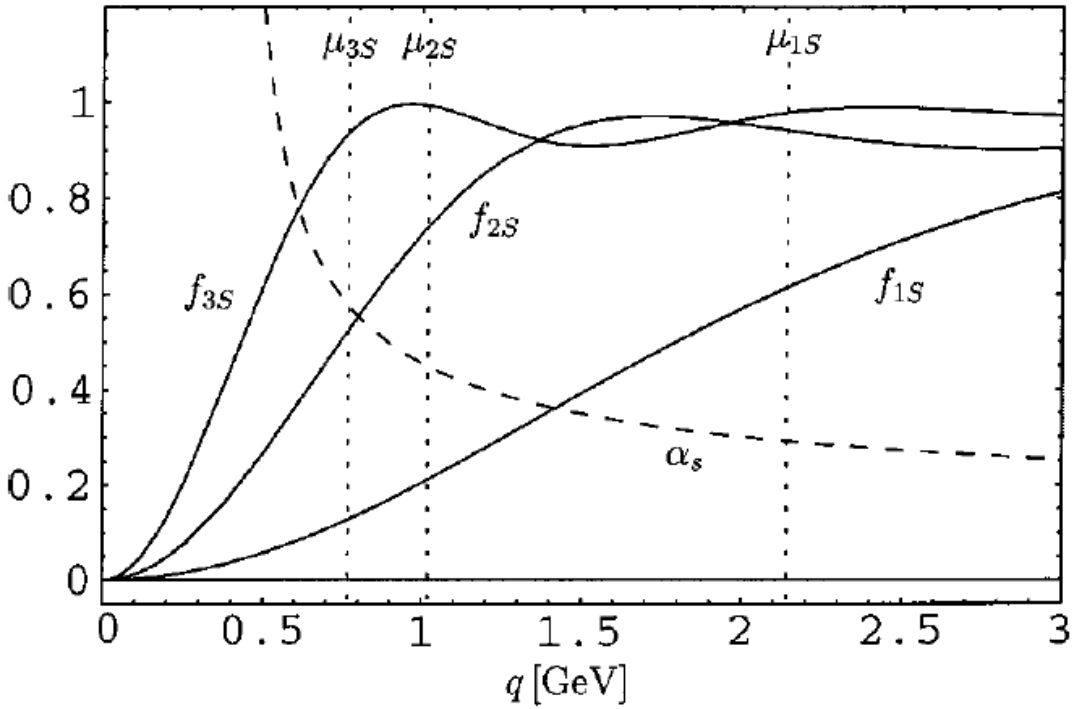

FIG. 5. Support functions for the S states. The solid curves show the support functions as defined in Eq. (19); for comparison of the relevant scales, $\alpha_s^{(4)}(\mu)$ is also plotted (dashed curve). Since the analysis that we advocate in this work does not attribute scales to the individual states, the scales indicated by the dotted lines are taken from [3], Table II.

Rapid growth of masses of excited states originates from rapid growth of self-energies of Q & $\overline{Q}$ due to IR gluons.

Brambilla, Y.S., Vairo

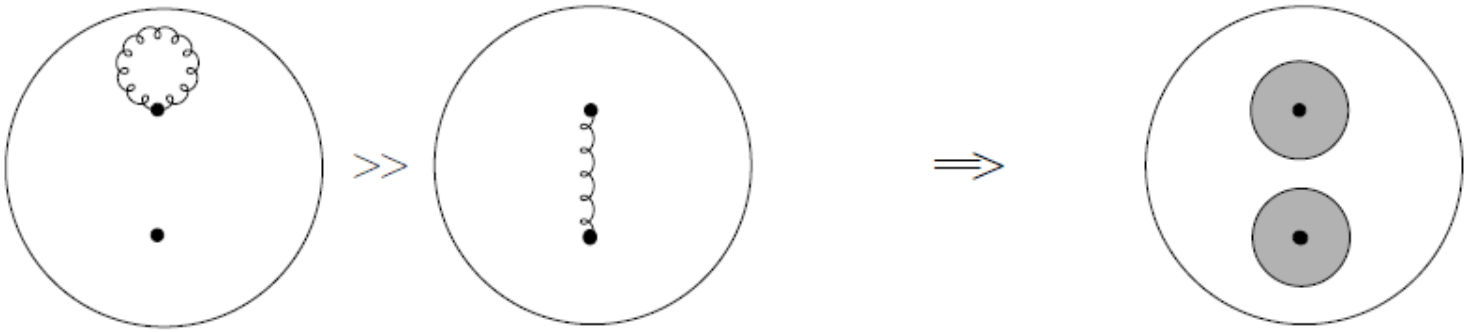

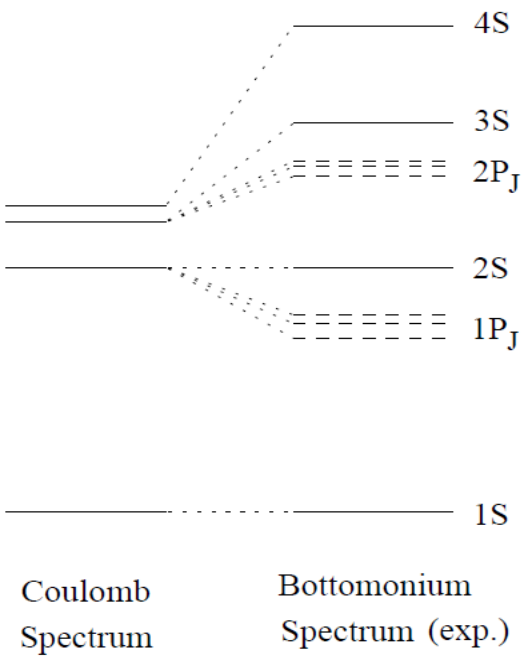

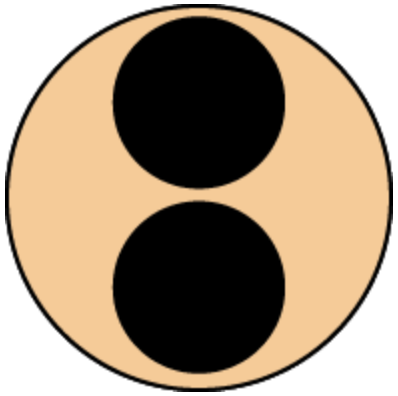

3. OPE of QCD potential $V_{\mathrm{QCD}}(r)$

What to do with residual $O(\Lambda^3 r^2)$ renormalon?

Solution

In OPE, IR renormalons in Wilson coeffs. should be separated and abosorbed into non-pert. matrix elements. Wilson; Müller

$$V_{\rm QCD}(r) = V_S(r)\cdot\langle \mathbf{1}\rangle + \text{const.} + \delta E_{US}(r) + \cdots$$

Brambilla,Pineda,Soto,Vairo

Wilson coeff

$$\delta E_{US}(r) = g^2 \int_0^\infty dt\, e^{-it\Delta V}\, \langle \vec{r}\cdot\vec{E}^a(t)\, \varphi_{ab}(t)\, \vec{r}\cdot\vec{E}^b(0)\rangle$$

non-pert. matrix element

"Contour-deformation prescription"

Expand in r: $V_C(r) + C_0^V\cdot\Lambda_{\rm QCD} + C_1^V\cdot\Lambda_{\rm QCD}^2 r + C_2^V\cdot\Lambda_{\rm QCD}^3 r^2 + \cdots$

YS, Takaura
Hayashi, YS, Takaura

Solution

In OPE, IR renormalons in Wilson coeffs. should be separated and abosorbed into non-pert. matrix elements.

Wilson; Müller

$$V_{\rm QCD}(r) = V_S(r)\cdot\langle \mathbf{1}\rangle + \text{const.} + \delta E_{US}(r) + \cdots$$

Brambilla,Pineda,Soto,Vairo

Wilson coeff

$$\delta E_{US}(r) = g^2 \int_0^\infty dt\, e^{-it\Delta V}\, \langle \vec{r}\cdot\vec{E}^a(t)\, \varphi_{ab}(t)\, \vec{r}\cdot\vec{E}^b(0)\rangle$$

non-pert. matrix element

"Contour-deformation prescription"

Expand in r: $V_C(r) + C_0^V\cdot\Lambda_{\rm QCD} + C_1^V\cdot\Lambda_{\rm QCD}^2 r + C_2^V\cdot\Lambda_{\rm QCD}^3 r^2 + \cdots$

renormalon renormalon

YS, Takaura
Hayashi, YS, Takaura

Solution

In OPE, IR renormalons in Wilson coeffs. should be separated and abosorbed into non-pert. matrix elements. Wilson; Müller

$$V_{\rm QCD}(r) = V_S(r)\cdot\langle \mathbf{1}\rangle + \text{const.} + \delta E_{US}\,(r) + \cdots$$

Brambilla,Pineda,Soto,Vairo

$$\| $$

$$g^2 \int_0^\infty dt\, e^{-it\Delta V}\, \left\langle \vec{r}\cdot\vec{E}^a(t)\, \varphi_{ab}(t)\, \vec{r}\cdot\vec{E}^b(0)\right\rangle$$

"Contour-deformation prescription"

Expand in r: $V_C(r) + C_0^V\cdot\Lambda_{\rm QCD} + C_1^V\cdot\Lambda_{\rm QCD}^2 r + C_2^V\cdot\Lambda_{\rm QCD}^3\, r^2 + \cdots$

YS, Takaura

Hayashi, YS, Takaura

renormalon renormalon

$$= V_S^{RF}(r)\cdot\langle \mathbf{1}\rangle + \text{const.} + \delta E_{US}^{RF}\,(r) + \cdots$$

Solution

In OPE, IR renormalons in Wilson coeffs. should be separated and abosorbed into non-pert. matrix elements.

Wilson; Müller

$$V_{\rm QCD}(r) = V_S(r)\cdot\langle \mathbf{1}\rangle + \text{const.} + \delta E_{US}\,(r) + \cdots$$

Brambilla,Pineda,Soto,Vairo

$$\| $$

$$g^2 \int_0^\infty dt\, e^{-it\Delta V}\, \left\langle \vec{r}\cdot\vec{E}^a(t)\, \varphi_{ab}(t)\, \vec{r}\cdot\vec{E}^b(0)\right\rangle$$

"Contour-deformation prescription"

Expand in r: $V_C(r) + C_0^V\cdot\Lambda_{\rm QCD} + C_1^V\cdot\Lambda_{\rm QCD}^2 r + C_2^V\cdot\Lambda_{\rm QCD}^3\, r^2 + \cdots$

YS, Takaura

Hayashi, YS, Takaura

renormalon

renormalon

$$= V_S^{RF}(r)\cdot\langle \mathbf{1}\rangle + \text{const.} + \delta E_{US}^{RF}\,(r) + \cdots$$

Solution

In OPE, IR renormalons in Wilson coeffs. should be separated and abosorbed into non-pert. matrix elements.

Wilson; Müller

$$V_{\rm QCD}(r) = V_S(r)\cdot\langle \mathbf{1}\rangle + \text{const.} + \delta E_{US}\,(r) + \cdots$$

$$\| $$

$$g^2 \int_0^\infty dt\, e^{-it\Delta V}\, \left\langle \vec{r}\cdot\vec{E}^a(t)\, \varphi_{ab}(t)\, \vec{r}\cdot\vec{E}^b(0)\right\rangle$$

"Contour-deformation prescription"

Expand in r: $V_C(r) + C_0^V\cdot\Lambda_{\rm QCD} + C_1^V\cdot\Lambda_{\rm QCD}^2 r + C_2^V\cdot\Lambda_{\rm QCD}^3\, r^2 + \cdots$

YS, Takaura

Hayashi, YS, Takaura

renormalon

renormalon

$$= V_S^{RF}(r)\cdot\langle \mathbf{1}\rangle + \text{const.} + \delta E_{US}^{RF}\,(r) + \cdots$$

compare

$V_{\rm latt}(r)$

Solution

In OPE, IR renormalons in Wilson coeffs. should be separated and abosorbed into non-pert. matrix elements.

Wilson; Müller

$$V_{\rm QCD}(r) = V_S(r)\cdot\langle \mathbf{1}\rangle + \text{const.} + \delta E_{US}(r) + \cdots$$

$$\| $$

$$g^2 \int_0^\infty dt\, e^{-it\Delta V} \left\langle \vec{r}\cdot\vec{E}^a(t)\, \varphi_{ab}(t)\, \vec{r}\cdot\vec{E}^b(0)\right\rangle$$

"Contour-deformation prescription"

Expand in r: $V_C(r) + C_0^V\cdot\Lambda_{\rm QCD} + C_1^V\cdot\Lambda_{\rm QCD}^2 r + C_2^V\cdot\Lambda_{\rm QCD}^3 r^2 + \cdots$

YS, Takaura

Hayashi, YS, Takaura

renormalon

renormalon

$$= V_S^{RF}(r)\cdot\langle \mathbf{1}\rangle + \text{const.} + \delta E_{US}^{RF}(r) + \cdots$$

$A_2 r^2$ or $A_2 r^2(1 + c\log r)$

fitting param.

compare

$V_{\rm latt}(r)$

Consistency with lattice results and α_s determination

Consistency check

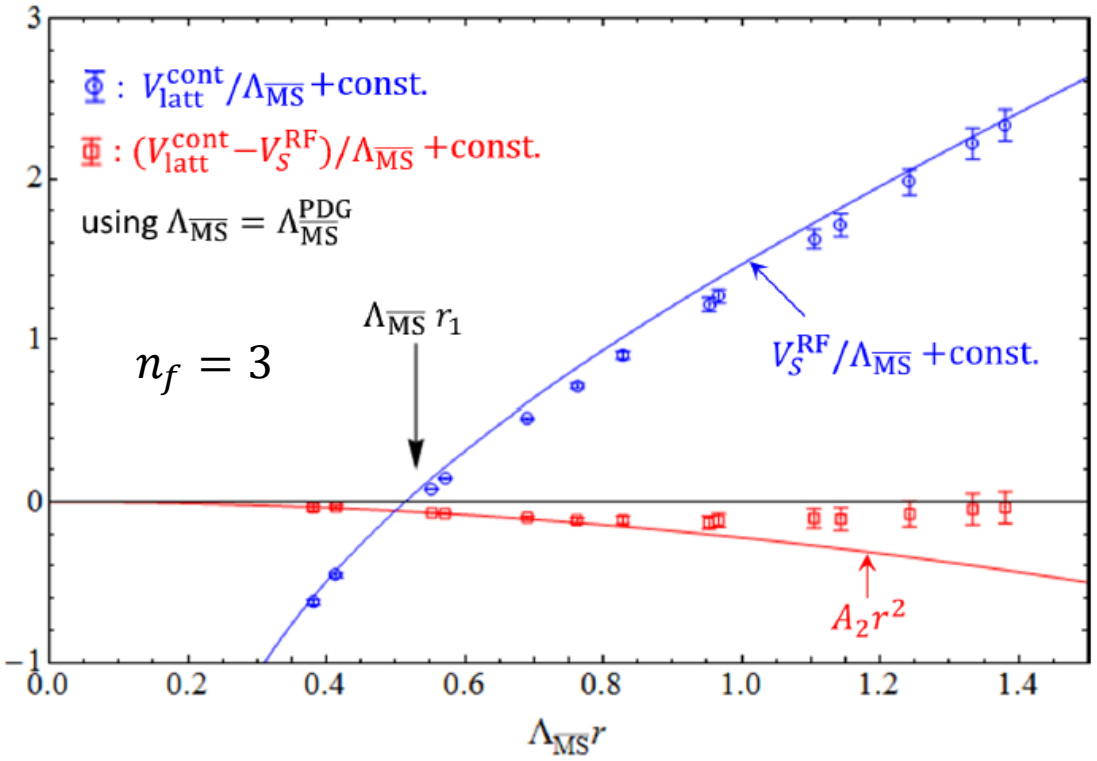

Takaura, Kaneko, Kiyo, YS

$$\alpha_s(M_Z) = 0.1179^{+0.0015}_{-0.0014}$$

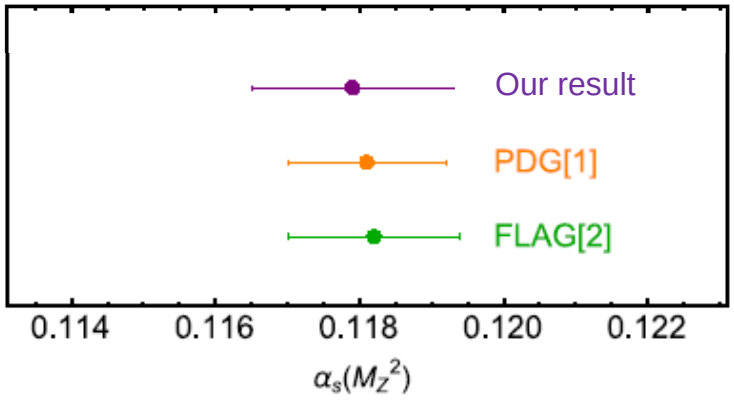

$V_{\rm QCD}(r)$ [JLQCD: after cont. limit] consistent with OPE at $r\Lambda_{\overline{MS}} \lesssim 0.8$ after renormalon subtraction.

First time to subtract NLO renormalon and confirm the OPE structure

$$V_{\rm QCD}(r) = V_S^{RF}(r) + V_{IR}^{RF}(r)$$

NNNLL fit fn: $A_0 + A_2 r^2$

4. After 1998: Many Applications

Spectroscopy

Decays

Determinations of m_b, m_c (m_t)

Determination of α_s

Gluon config. inside quarkonium

Casimir scaling violation for static potential

⋮

☆Summary

1. Before 1998: Theoretical problem

   IR ambiguity (renomalon)

2. Around 1998: Drastic improvement

   Discovery of cancellation of renormalons

   Interpretation

3. After 1998: Applications

   Spectroscopy

   Decays

   Determinations of m_b, m_c (m_t)

   Determination of α_s

   Gluon config. inside quarkonium

   Casimir scaling violation for static potential

   ⋮

☆Summary

OPE with subtraction of renormalons $\Rightarrow$ α_s determination

- OPE of $V_{\rm QCD}(r)$
- RG improvement of $V_S(r)$

Short-distance expansion

combines with non-pert. matrix element

$$V_{\rm QCD}(r) \sim \frac{c_{-1}}{r} + c_0 + c_1 r + c_2 r^2 + \cdots \quad \text{at } r \ll \Lambda_{\rm QCD}^{-1}$$

Genuinely UV contr. $V_S^{RF}(r)$ (renormalon-free) of pert. prediction separated.

First observation of OPE structure at $r\Lambda_{\overline{MS}} \lesssim 0.8$.

$$\alpha_s(M_Z) = 0.1179^{+0.0015}_{-0.0014}$$

Error reducible by finer lattices.

Backup Slides

Comparison with other methods

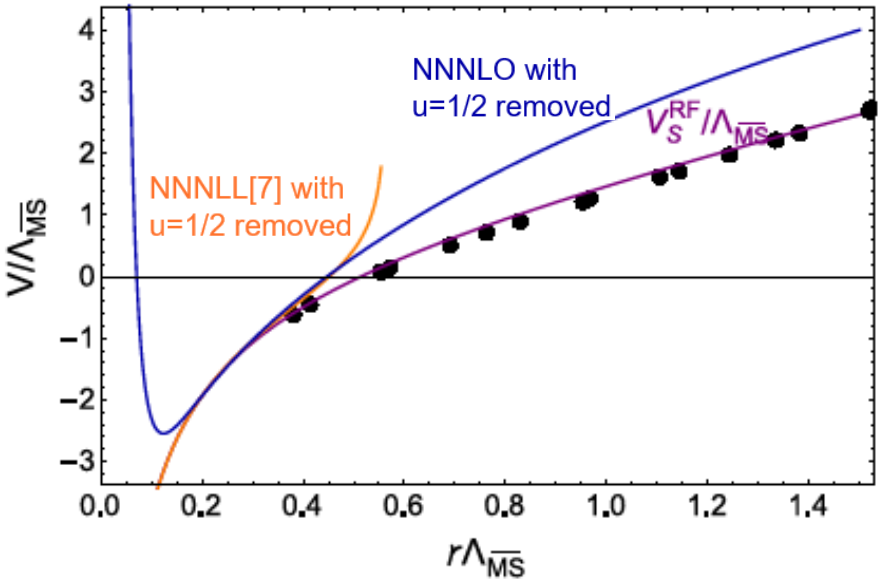

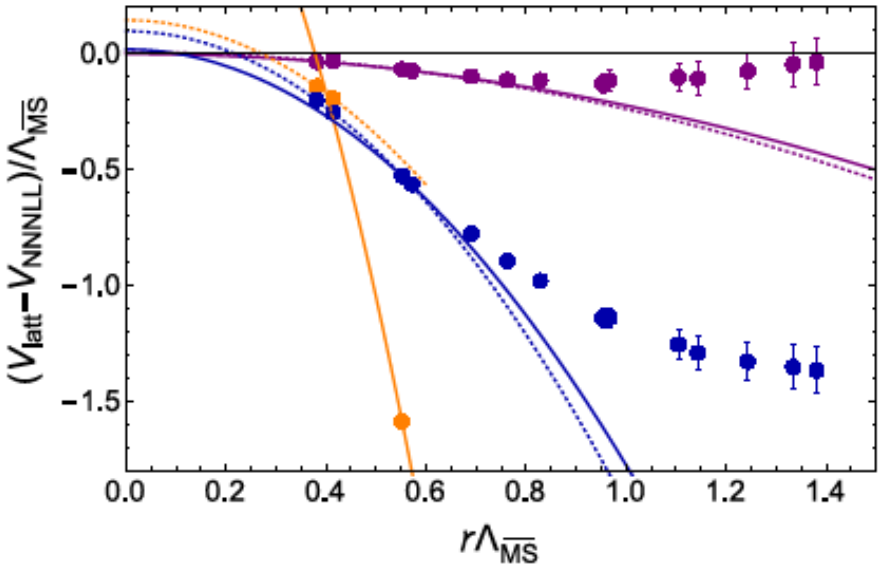

[7] Bazavov, Brambilla, Garcia i Tormo, Petreczky, Soto, Vairo

Scale dep. is much smaller compared to other methods.

r^2 behavior stably observed up to larger distances.

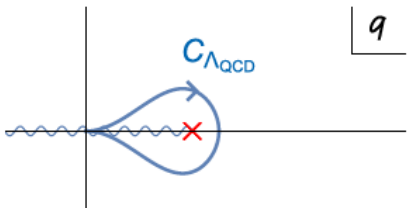

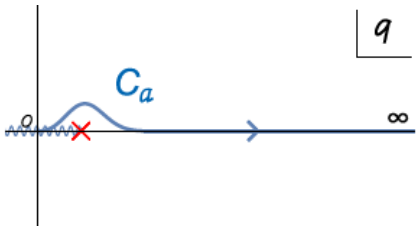

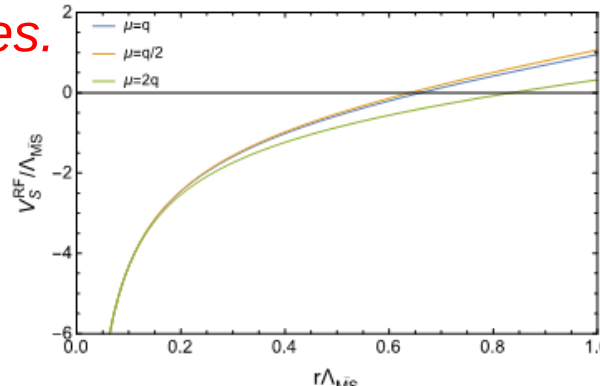

The case of $V_{\rm QCD}(r)$

It has been known that $V_{\rm QCD}(r)$ is plagued by renormalons, whereas its Fourier transf. $\tilde{V}_{\rm QCD}(q)$ is not.

Defined via Borel transf.

A new justification:

$$\tilde{V}_{\rm QCD}(q) = \int d^3\vec{r}\; e^{i\vec{q}\cdot\vec{r}}\, V_{\rm QCD}(r) \quad \Rightarrow \quad \delta\tilde{V}_{\rm QCD}(q) = \int d^3\vec{r}\; e^{i\vec{q}\cdot\vec{r}}\, \delta V_{\rm QCD}(r)$$

$$\delta V_{\rm QCD}(r) = N(u_*)\, r^{-1}\left(r\Lambda_{\rm QCD}\right)^{2u_*} \quad \text{by renormalon at } u = u_*$$

$$\Rightarrow \quad \delta\tilde{V}_{\rm QCD}(q) = N(u_*)\, q^{-2}\left(\Lambda_{\rm QCD}/q\right)^{2u_*}\, \Gamma(2u_*+1)\, \underline{\cos(\pi u_*)}$$ YS, Takaura

Renormalons vanish at $u = \frac{1}{2}, \frac{3}{2}, \frac{5}{2}, \cdots$ *!*

Separation and subtraction of renormalons:

$$V_{\rm QCD}(r) = \int \frac{d^3\vec{q}}{(2\pi)^3}\, e^{-i\vec{q}\cdot\vec{r}}\, \tilde{V}_{\rm QCD}(q) = \frac{1}{2\pi^2}\int_0^\infty dq\, \frac{\sin qr}{qr}\, \tilde{V}_{\rm QCD}(q)$$

$$\left[V_{\rm QCD}(r)\right]_{R-\rm subt.} = \frac{1}{2\pi^2}\,\Pr.\int_0^\infty dq\, \frac{\sin qr}{qr}\left[\tilde{V}_{\rm QCD}(q)\right]_{RG-\rm imp.}$$

Coincides with the expression used e.g. in α_s-determination by Takaura, et al. (2018)

Renormalon uncertainty

't Hooft

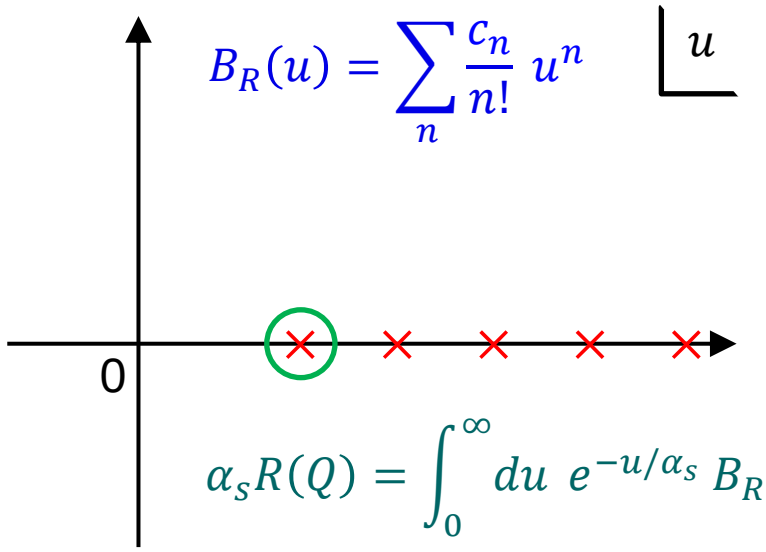

Later it was shown that renormalon uncertainties can be absorbed into non-pert. matrix elements in OPE.

Mueller

$$R(Q) \propto \int_0^Q dq\, q^P \alpha_s(q) = \sum_n c_n\, \alpha_s^n(\mu)$$

$$\alpha_s(q) = \frac{\alpha_s(\mu)}{1 - b_0 \alpha_s(\mu) \log(\mu/q)}$$

with $c_n \sim n!$

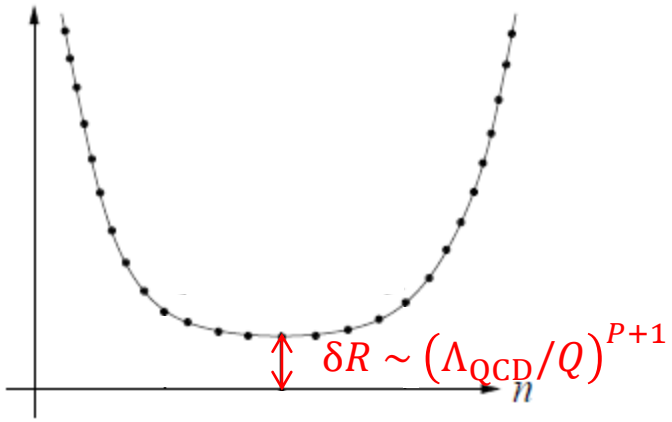

Asymptotic series ⇨ Limited accuracy

Short-distance expansion of $V_{\rm QCD}(r)$ (qualitative)

$$V_{\rm QCD}(r) \sim \frac{c_{-1}}{r} + c_0 + c_1 r + c_2\, r^2 + \cdots \qquad \text{at } r \ll \Lambda_{\rm QCD}^{-1}$$

IR renormalons in pert. QCD prediction

$O(\Lambda)$ $\quad$ $O(\Lambda^3 r^2)$

⇩

OPE of QCD potential in Potential-NRQCD

multipole expansion in $\vec{r}$

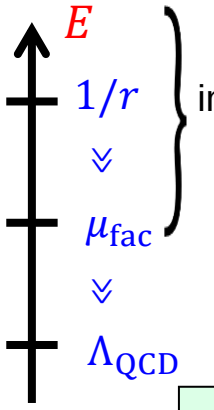

integrated out

Brambilla, Pineda, Soto, Vairo

Uncertainty in $c_2\, r^2$ replaced by a non-pert. matrix element.

$$V_{\rm QCD}(r) = \underbrace{V_{UV}(r;\mu_{\rm fac})}_{\text{UV contr.}} + \underbrace{V_{IR}(r;\mu_{\rm fac})}_{\text{IR contr.}}$$

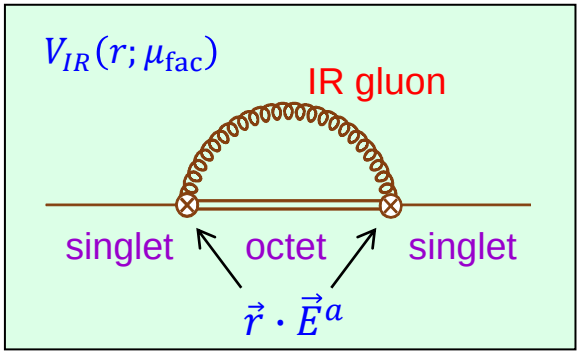

$$V_{IR}(r;\mu_{\rm fac}) = g^2 \int_0^\infty dt\, e^{-it\Delta V} \left\langle \vec{r}\cdot\vec{E}^a(t)\, \varphi_{ab}(t)\, \vec{r}\cdot\vec{E}^b(0)\right\rangle + O(r^3)$$

UV contribution

$$V_{\rm UV}(r;\mu_f) \equiv -\int_{q>\mu_f} \frac{d^3\vec{q}}{(2\pi)^3}\, e^{i\vec{q}\cdot\vec{r}}\, C_F \frac{4\pi\alpha_{\rm 1L}(q)}{q^2}$$

$$\alpha_{\rm 1L}(q) = \frac{2\pi}{\beta_0 \log\left(q/\Lambda_{\rm QCD}\right)} \quad : \text{LL resum.}$$

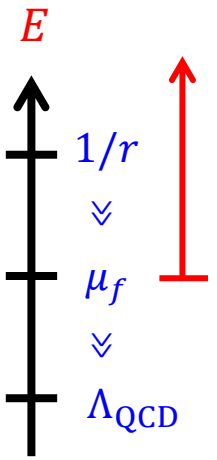

We can separate μ_f -dependent and μ_f -independent parts as follows.

$$V_{\rm UV}(r;\mu_f) \overset{\int d\Omega_{\vec{q}}}{=} -\frac{2C_F}{\pi}\int_{\mu_f}^{\infty} dq\, \frac{\sin(qr)}{qr}\,\alpha_{\rm 1L}(q) = -\frac{2C_F}{\pi}{\rm Im}\int_{\mu_f}^{\infty} dq\, \frac{e^{iqr}}{qr}\,\alpha_{\rm 1L}(q)$$

UV contribution

$$V_{\rm UV}(r;\mu_f) \equiv -\int_{q>\mu_f} \frac{d^3\vec{q}}{(2\pi)^3}\, e^{i\vec{q}\cdot\vec{r}}\, C_F \frac{4\pi\alpha_{\rm 1L}(q)}{q^2}$$

$$\alpha_{\rm 1L}(q) = \frac{2\pi}{\beta_0 \log\left(q/\Lambda_{\rm QCD}\right)} \quad : \text{LL resum.}$$

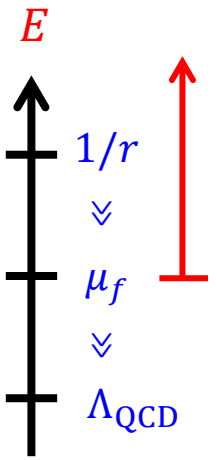

We can separate μ_f -dependent and μ_f -independent parts as follows.

$$V_{\rm UV}(r;\mu_f) \overset{\int d\Omega_{\vec{q}}}{=} -\frac{2C_F}{\pi}\int_{\mu_f}^{\infty} dq\, \frac{\sin(qr)}{qr}\,\alpha_{\rm 1L}(q) = -\frac{2C_F}{\pi}\,{\rm Im}\underbrace{\int_{\mu_f}^{\infty} dq\, \frac{e^{iqr}}{qr}}_{C_1 - C_3}\,\alpha_{\rm 1L}(q)$$

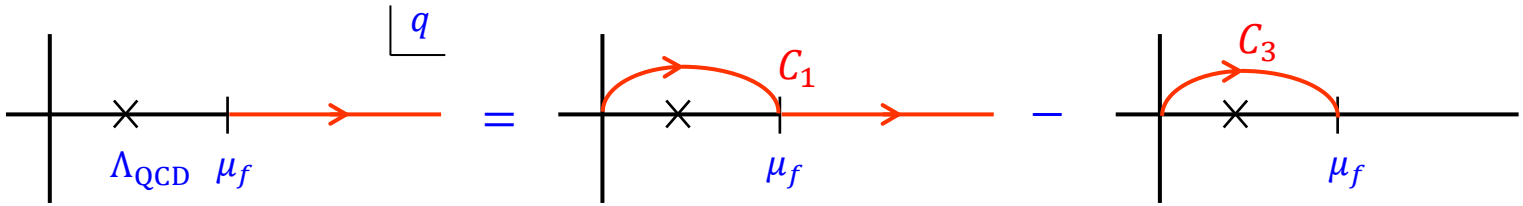

UV contribution

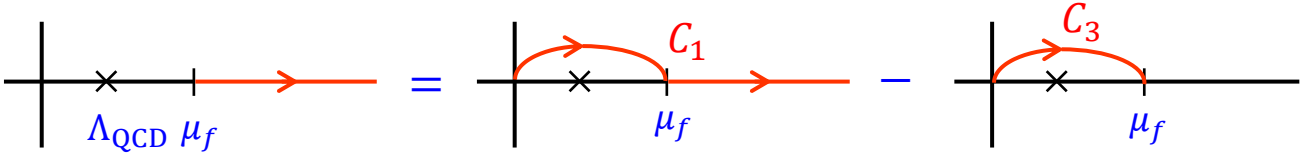

$$V_{UV}(r;\mu_f) = -\frac{2C_F}{\pi}\,\mathrm{Im}\int_{C_1} dq\,\frac{e^{iqr}}{qr}\,\alpha_{1L}(q) + \frac{2C_F}{\pi}\,\mathrm{Im}\int_{C_3} dq\,\frac{e^{iqr}}{qr}\,\alpha_{1L}(q)$$

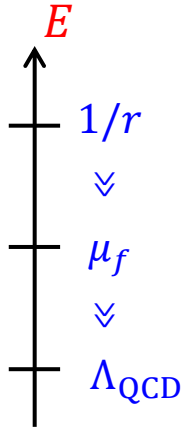

- Along C_3, justified to expand e^{iqr} in iqr, since $\mu_f r \ll 1$:

$$\frac{2C_F}{\pi}\mathrm{Im}\int_{C_3} dq\,\frac{1+iqr+\frac{1}{2}(iqr)^2+\cdots}{qr}\,\alpha_{1\mathrm{L}}(q) = \frac{A}{r} + B + \sigma r + Dr^2 + \mathcal{O}(r^3)$$

A and σ can be computed analytically.

UV contribution

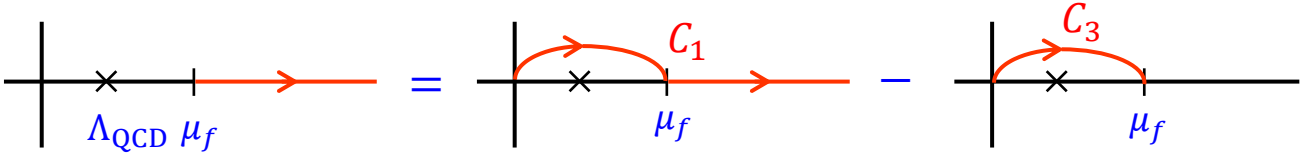

$$V_{UV}(r;\mu_f) = -\frac{2C_F}{\pi}\,\mathrm{Im}\int_{C_1} dq\,\frac{e^{iqr}}{qr}\,\alpha_{1L}(q) + \frac{2C_F}{\pi}\,\mathrm{Im}\int_{C_3} dq\,\frac{e^{iqr}}{qr}\,\alpha_{1L}(q)$$

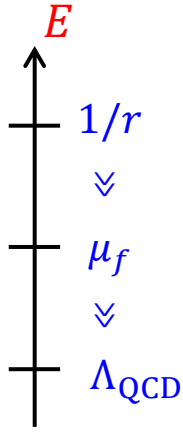

- Along C_3, justified to expand e^{iqr} in iqr, since $\mu_f r \ll 1$:

$$\frac{2C_F}{\pi}\mathrm{Im}\int_{C_3} dq\,\frac{1+iqr+\frac{1}{2}(iqr)^2+\cdots}{qr}\,\alpha_{1\mathrm{L}}(q) = \frac{A}{r} + B + \sigma r + Dr^2 + \mathcal{O}(r^3)$$

A and σ can be computed analytically:

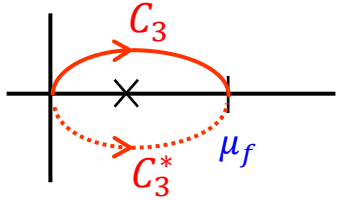

$$A = \frac{2C_F}{\pi}\mathrm{Im}\int_{C_3} dq\,\frac{\alpha_{1\mathrm{L}}(q)}{q} = \frac{C_F}{\pi i}\int_{C_3-C_3^*} dq\,\frac{\alpha_{1\mathrm{L}}(q)}{q}$$

$$= -\frac{C_F}{\pi i}\int_{C_2} dq\,\frac{\alpha_{1\mathrm{L}}(q)}{q} = -\frac{4\pi C_F}{\beta_0}.$$

↑ Cauchy thm

μ_f *independent !*

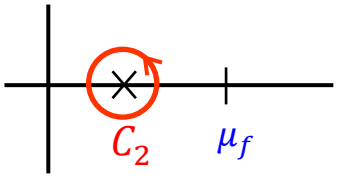

$$\sigma = \frac{2C_F}{\pi}\mathrm{Im}\int_{C_3} dq\left(-\frac{1}{2}q\right)\alpha_{1\mathrm{L}}(q) = \frac{C_F}{2\pi i}\int_{C_2} dq\,q\,\alpha_{1\mathrm{L}}(q) = \frac{2\pi C_F}{\beta_0}\Lambda_{\mathrm{QCD}}^2$$

UV contribution

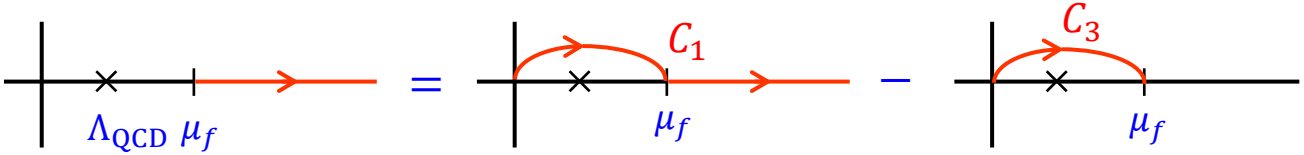

$$V_{UV}(r;\mu_f) = -\frac{2C_F}{\pi}\,\mathrm{Im}\int_{C_1} dq\,\frac{e^{iqr}}{qr}\,\alpha_{1L}(q) + \frac{2C_F}{\pi}\,\mathrm{Im}\int_{C_3} dq\,\frac{e^{iqr}}{qr}\,\alpha_{1L}(q)$$

$$= V_C(r) + B + \sigma r + Dr^2 + O(r^3)$$

μ_f independent

$$V_C(r) = \frac{A}{r} - \frac{2C_F}{\pi}\,\mathrm{Im}\int_{C_1} dq\,\frac{e^{iqr}}{qr}\,\alpha_{1\mathrm{L}}(q).$$

$$V_C(r) \to \begin{cases} -\dfrac{2\pi C_F}{\beta_0}\,\dfrac{1}{r\left|\log(\Lambda_{\rm QCD}\, r)\right|}, & r \to 0, \\ -\dfrac{4\pi C_F}{\beta_0 r}, & r \to \infty. \end{cases}$$

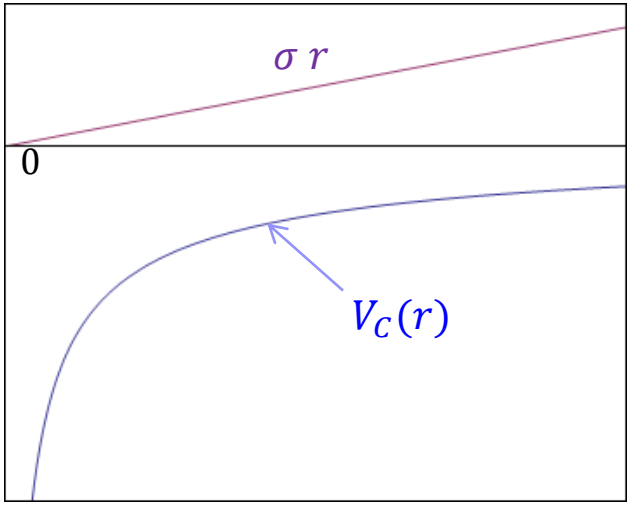

UV contribution

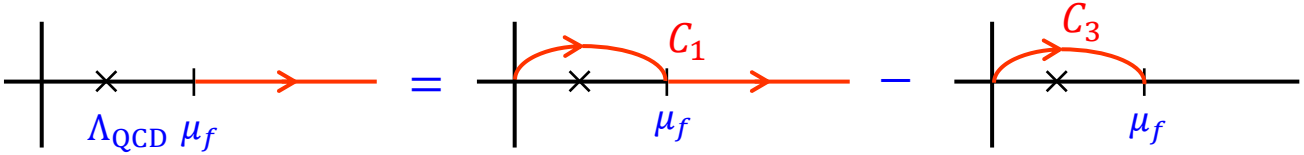

$$V_{UV}(r;\mu_f) = -\frac{2C_F}{\pi}\,\mathrm{Im}\int_{C_1} dq\,\frac{e^{iqr}}{qr}\,\alpha_{1L}(q) + \frac{2C_F}{\pi}\,\mathrm{Im}\int_{C_3} dq\,\frac{e^{iqr}}{qr}\,\alpha_{1L}(q)$$

$$= V_C(r) + B + \sigma r + Dr^2 + O(r^3) \quad \Leftarrow$$

A short-distance expansion in r with correct RG log in Coulomb term (as $r \to 0$)

μ_f independent

$$V_C(r) = \frac{A}{r} - \frac{2C_F}{\pi}\,\mathrm{Im}\int_{C_1} dq\,\frac{e^{iqr}}{qr}\,\alpha_{1\mathrm{L}}(q).$$

$$V_C(r) \to \begin{cases} -\dfrac{2\pi C_F}{\beta_0}\,\dfrac{1}{r\left|\log(\Lambda_{\rm QCD}\, r)\right|}, & r \to 0, \\ -\dfrac{4\pi C_F}{\beta_0 r}, & r \to \infty. \end{cases}$$

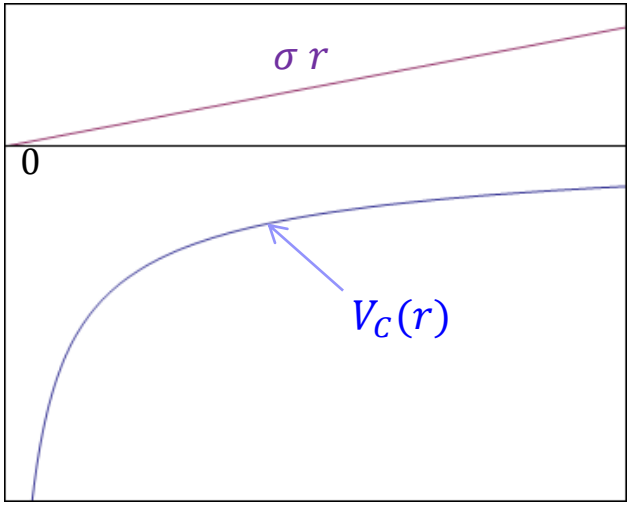

$$V_{\rm UV}(r;\mu_f)$$

$$V_{\rm QCD}(r) = \text{const.} + \underbrace{V_C(r) + \sigma r}_{\mu_f\text{-indep.}} + \underbrace{Dr^2 + V_{\rm IR}^{(\rm LO)}(r;\mu_f)}_{\mu_f\text{-indep.}} + \mathcal{O}(r^3).$$

genuinely UV $O(\Lambda^3 r^2)$ renormalons cancel

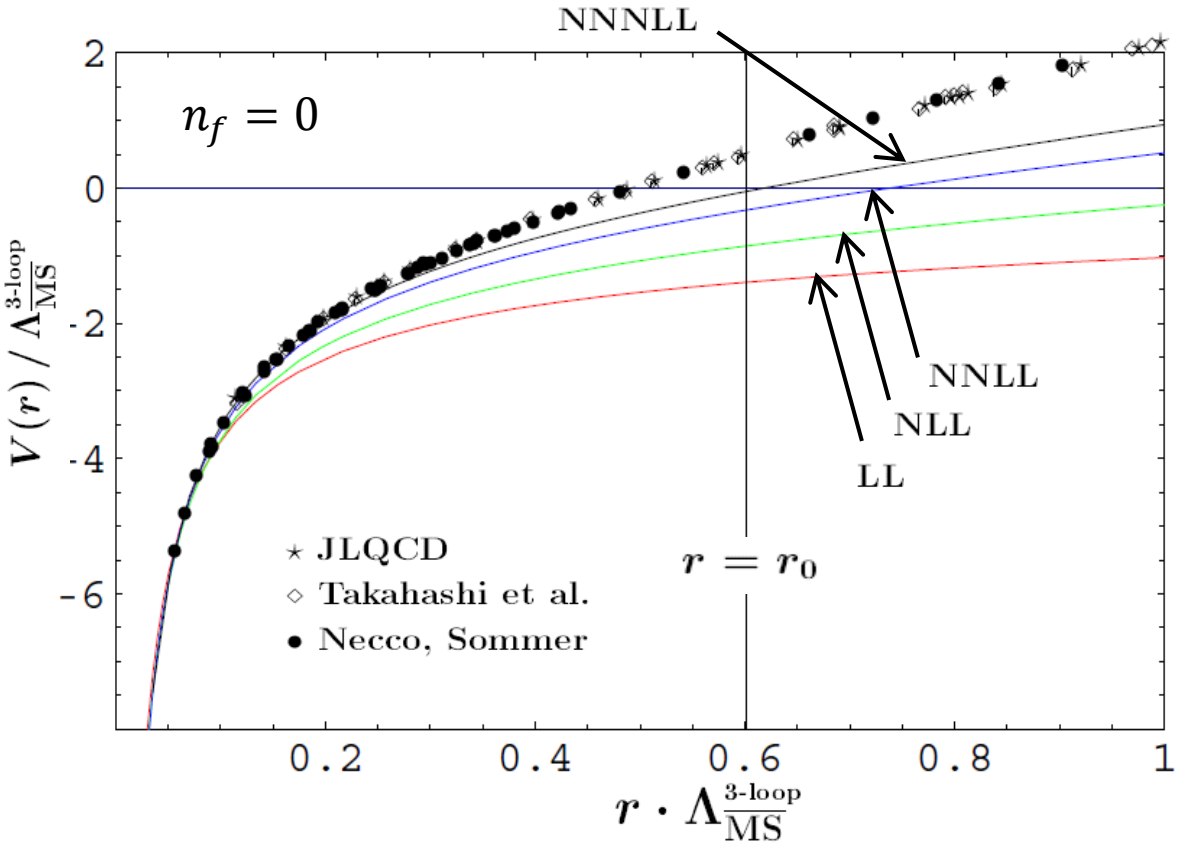

$V_C(r) + \sigma r$ including subleading logs vs. lattice comp.

hep-ph/0505034

$$V_{\rm QCD}(r) = \text{const.} + \overbrace{\underbrace{V_C(r) + \sigma r}_{\mu_f\text{-indep.}} + \underbrace{Dr^2 + V_{\rm IR}^{(\rm LO)}(r;\mu_f)}_{\mu_f\text{-indep.}}}^{V_{\rm UV}(r;\mu_f)} + \mathcal{O}(r^3).$$

genuinely UV

$O(\Lambda^3 r^2)$ renormalons cancel

each combination is renormalon-free

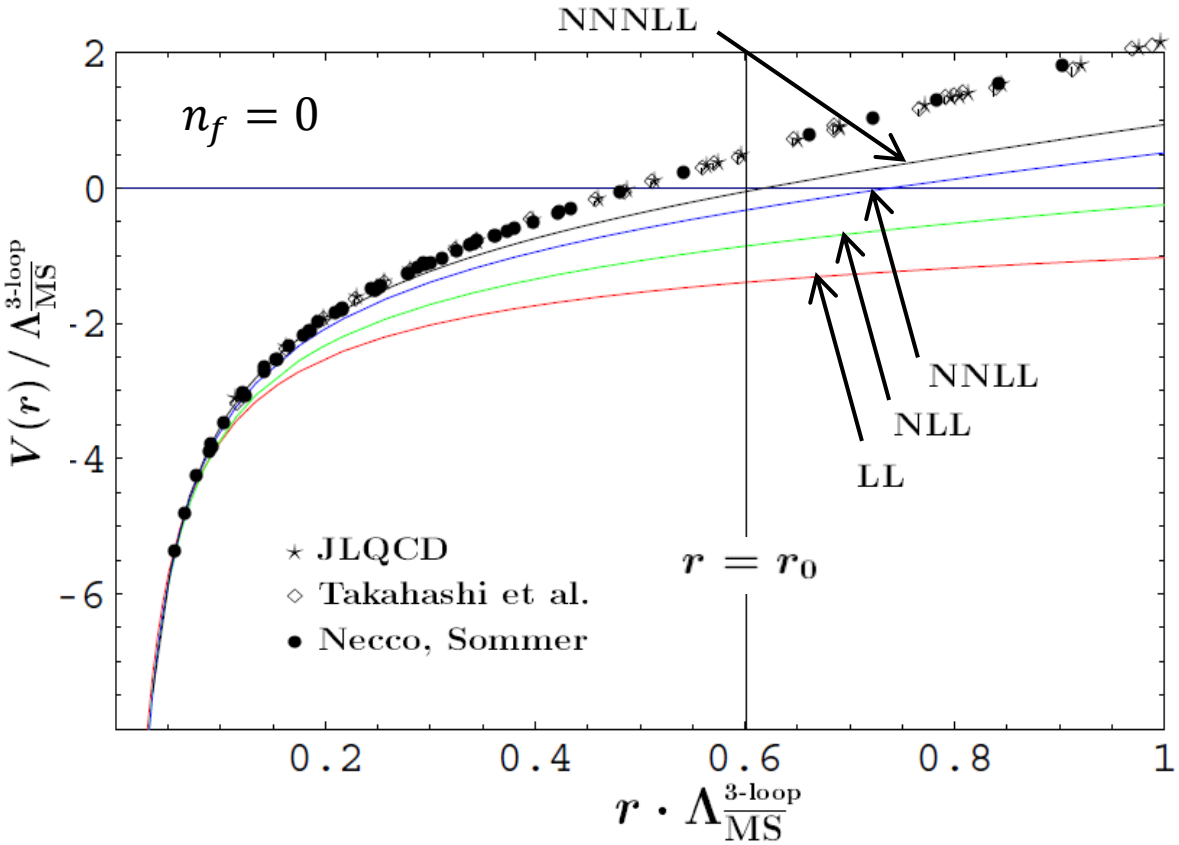

$V_C(r) + \sigma r$ including subleading logs vs. lattice comp.

arXiv:1411.7853

Interpretation of $V_C(r) + \sigma r$

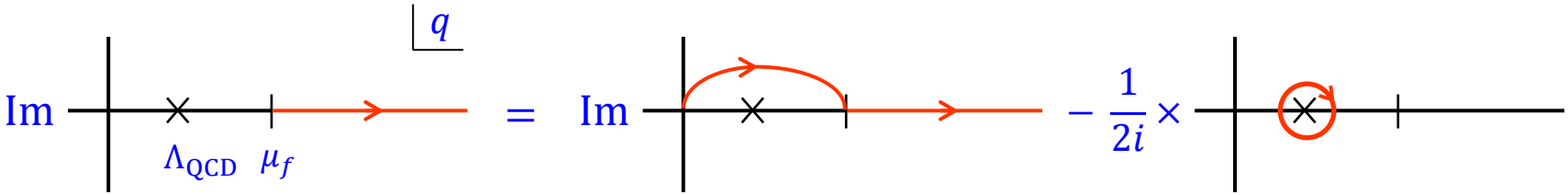

Contributions from IR region subtracted as contour integrals surrounding pole (singularity) at $q = \Lambda_{\rm QCD}$.

Can be regarded as generalization of ``integration-by-regions'' technique.

“Integration-by-regions” method

Simplified example:

$$\int_0^\infty dp \, \frac{p^\epsilon}{(p+m)(p+1)} \qquad m \ll 1 \, (= M)$$

“Integration-by-regions” method

Simplified example:

$$\int_0^\infty dp\,\frac{p^\varepsilon}{(p+m)(p+1)} \qquad m \ll 1\,(=M)$$

$$= \underbrace{\int_0^\infty dp\,\frac{p^\varepsilon}{p+m}\,(1-p+p^2+\cdots)}_{p \ll 1} + \underbrace{\int_0^\infty dp\,\frac{p^\varepsilon}{p+1}\,\frac{1}{p}\left(1-\frac{m}{p}+\cdots\right)}_{p \gtrsim 1 \gg m}$$

“Integration-by-regions” method

Simplified example:

$$\int_0^\infty dp\,\frac{p^\varepsilon}{(p+m)(p+1)} \qquad m \ll 1\,(=M)$$

$$= \int_0^\infty dp\,\frac{p^\varepsilon}{p+m}\,(1-p+p^2+\cdots) + \int_0^\infty dp\,\frac{p^\varepsilon}{p+1}\,\frac{1}{p}\left(1-\frac{m}{p}+\cdots\right)$$

$p \ll 1$ $\qquad$ $p \gtrsim 1 \gg m$

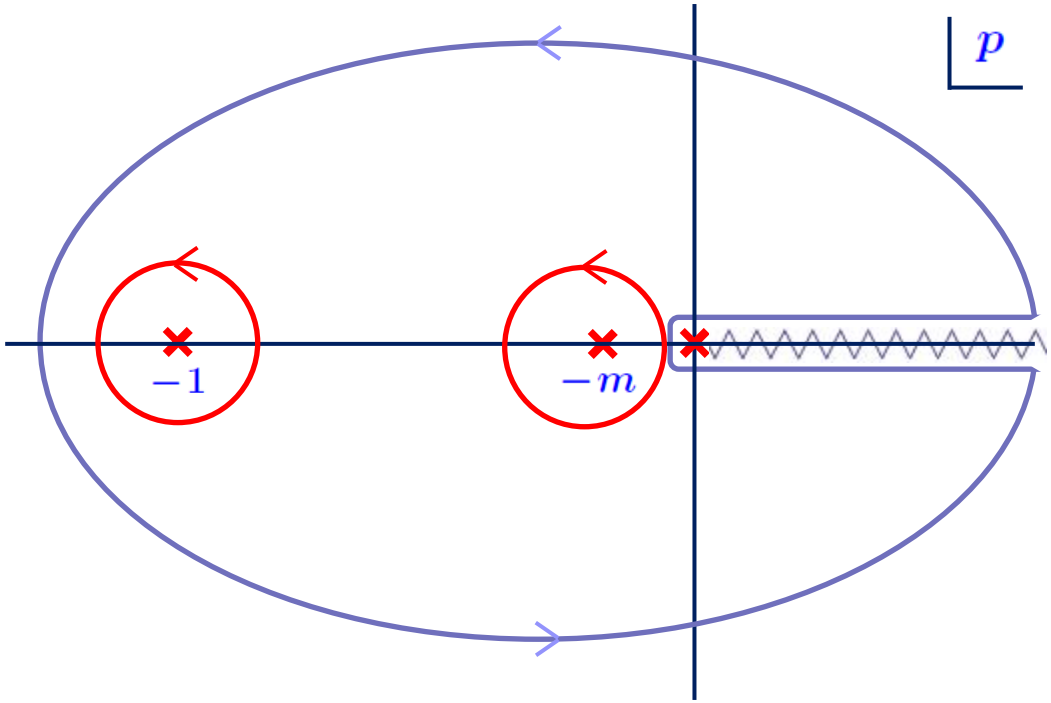

"Integration-by-regions" method

Simplified example:

$$\int_0^\infty dp\,\frac{p^\epsilon}{(p+m)(p+1)} \qquad m \ll 1\,(=M)$$

$$= \int_0^\infty dp\,\frac{p^\epsilon}{p+m}\,(1-p+p^2+\cdots) + \int_0^\infty dp\,\frac{p^\epsilon}{p+1}\,\frac{1}{p}\left(1-\frac{m}{p}+\cdots\right)$$

$p \ll 1$ $\qquad$ $p \gtrsim 1 \gg m$

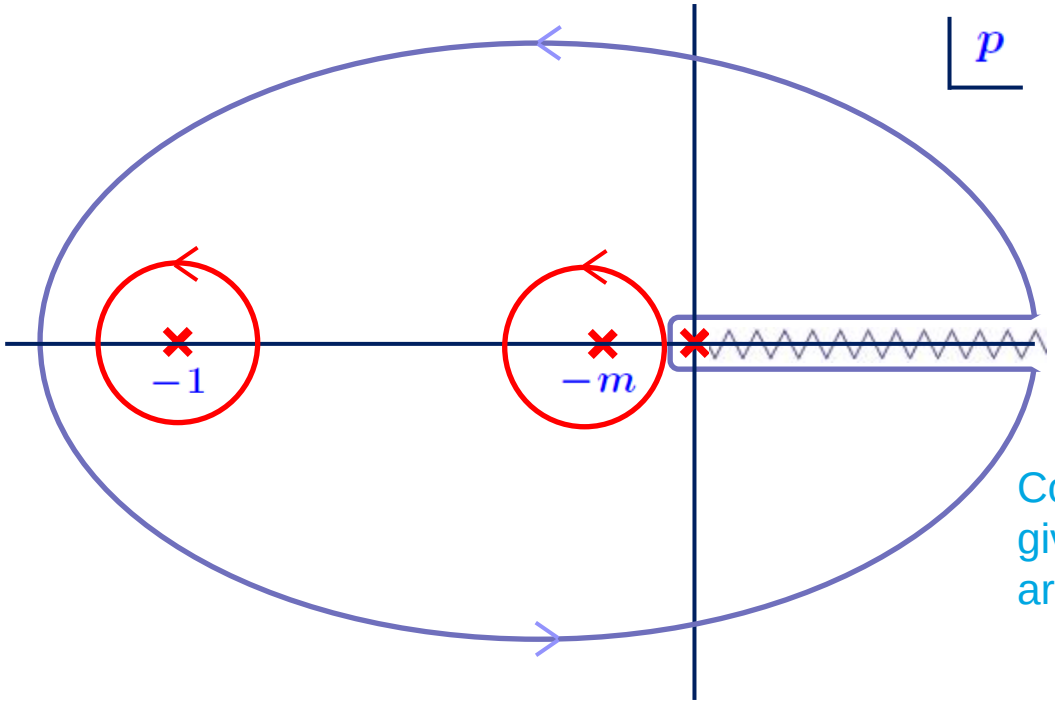

Contribution of each scale given by contour integral around singularity

4. After 1998: Many Applications

Spectroscopy

Decays

Determinations of m_b, m_c (m_t)

Determination of α_s

Gluon config. inside quarkonium

Casimir scaling violation for static potential

⋮

Application to quarkonium spectroscopy and determination of α_s, m_b, m_c.

- Global level structure of bottomonium is reproduced. Brambilla, Y.S., Vairo Recksiegel, Y.S
- Fine and hyperfine splittings of charmonium/bottomonium reproduced.
  Two exceptions in ~2003: Recksiegel, Y.S.; Kniehl, Penin, Pineda, Smirnov, Steinhauser
  charmonium hyperfine splitting $\Psi(2S)$–$\eta_c(2S)$
  bottomonium hyperfine splitting $\Upsilon(1S)$–$\eta_b(1S)$
  Solved in favor of pert. QCD predictions.
- Determination of bottom and charm quark $\overline{\text{MS}}$ masses:

$$\overline{m}_b(\overline{m}_b) = 4190 \pm 30 \text{ MeV}$$
$$\overline{m}_c(\overline{m}_c) = 1243 \pm 100 \text{ MeV}$$

Brambilla, Y.S., Vairo

- Relation between lattice α_s and $\overline{\text{MS}}$ α_s being accurately measured
  (realistic precision determination in near future) Y.S. Brambilla, Petreczky, Tormo, Soto, Vairo

Bottomonium spectrum up to $n = 3$ states

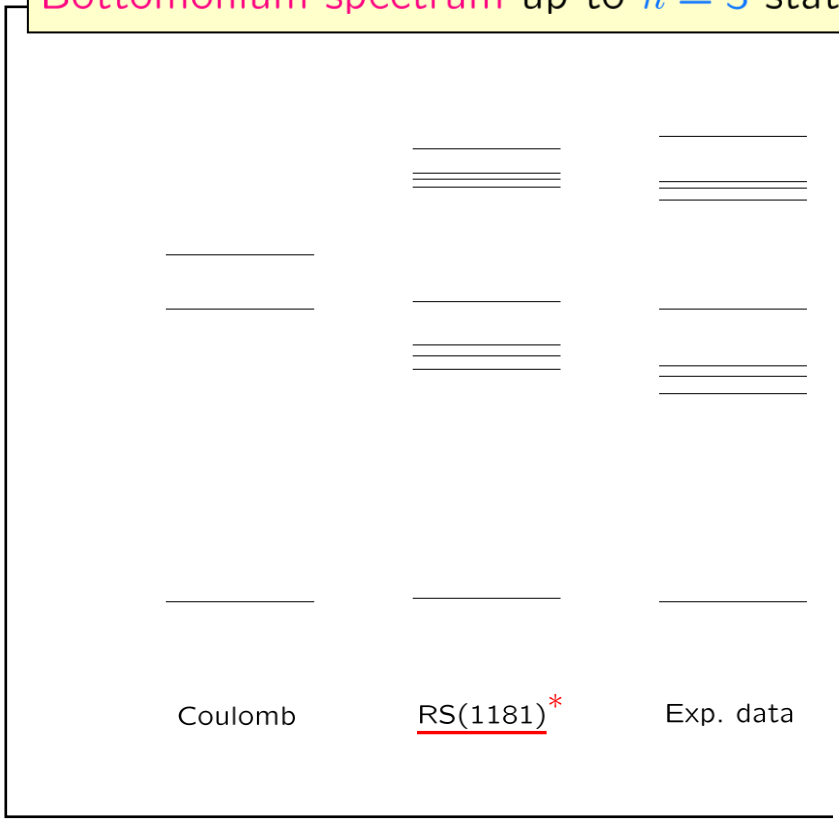

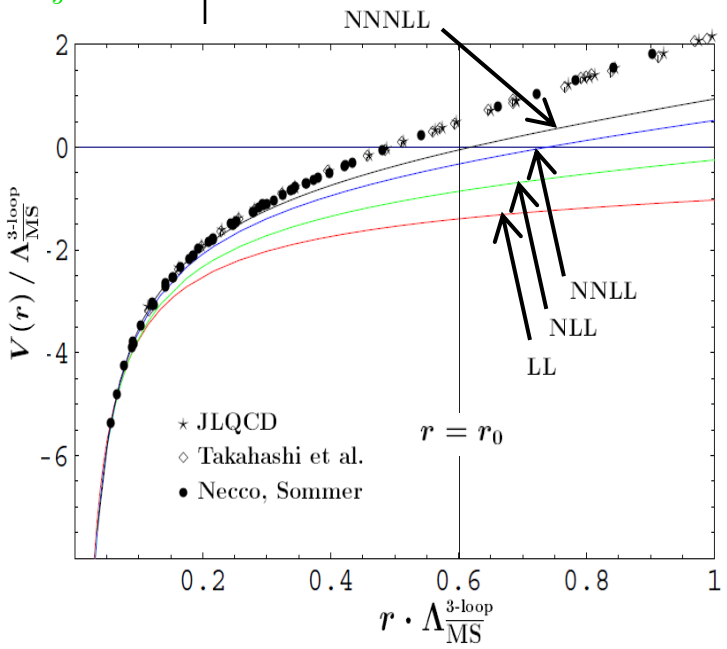

* Pert. QCD prediction including full $\mathcal{O}(\alpha_S^4 m)$ corrections to individual energy levels, as well as full $\mathcal{O}(\alpha_S^5 m)$ corrections to fine structure [$\alpha_S(M_Z) = 0.1181$]. Recksiegel, Y.S.

Application to quarkonium spectroscopy and determination of α_s, m_b, m_c.

- Global level structure of bottomonium is reproduced. Brambilla, Y.S., Vairo
  Recksiegel, Y.S

- Fine and hyperfine splittings of charmonium/bottomonium reproduced.
  Two exceptions in ~2003: Recksiegel, Y.S.; Kniehl, Penin,
  charmonium hyperfine splitting $\Psi(2S)$–$\eta_c(2S)$ Pineda, Smirnov, Steinhauser
  bottomonium hyperfine splitting $\Upsilon(1S)$–$\eta_b(1S)$
  Solved in favor of pert. QCD predictions.

- Determination of bottom and charm quark $\overline{\text{MS}}$ masses:

$$\overline{m}_b(\overline{m}_b) = 4190 \pm 30 \text{ MeV}$$
$$\overline{m}_c(\overline{m}_c) = 1243 \pm 100 \text{ MeV}$$

  Brambilla, Y.S., Vairo

- Relation between lattice α_s and $\overline{\text{MS}}$ α_s being accurately measured
  (realistic precision determination in near future) Y.S.
  Brambilla, Petreczky, Tormo, Soto, Vairo

Application to quarkonium spectroscopy and determination of α_s, m_b, m_c.

- Global level structure of bottomonium is reproduced. Brambilla, Y.S., Vairo
  Recksiegel, Y.S

- Fine and hyperfine splittings of charmonium/bottomonium reproduced.
  Two exceptions in ~2003: Recksiegel, Y.S.; Kniehl, Penin,
  charmonium hyperfine splitting $\Psi(2S)$–$\eta_c(2S)$ Pineda, Smirnov, Steinhauser
  bottomonium hyperfine splitting $\Upsilon(1S)$–$\eta_b(1S)$
  Solved in favor of pert. QCD predictions.

- Determination of bottom and charm quark $\overline{\text{MS}}$ masses:

$$\overline{m}_b(\overline{m}_b) = 4190 \pm 30 \text{ MeV}$$
$$\overline{m}_c(\overline{m}_c) = 1243 \pm 100 \text{ MeV}$$

  Brambilla, Y.S., Vairo

- Relation between lattice α_s and $\overline{\text{MS}}$ α_s being accurately measured
  (realistic precision determination in near future) Y.S.
  Brambilla, Petreczky, Tormo, Soto, Vairo

Slides from Skwarnicki's plenary talk at Lepton-Photon 2003

Predictions for hyperfine splitting ratio

- For 20 years theorists were exposed to the experimental value of $\Delta M_{2S}=M(\psi(2S))-M(\eta_c(2S))$ which was wrong by a factor of 2
- Predictions for $\Delta M_{2S}/\Delta M_{1S}$

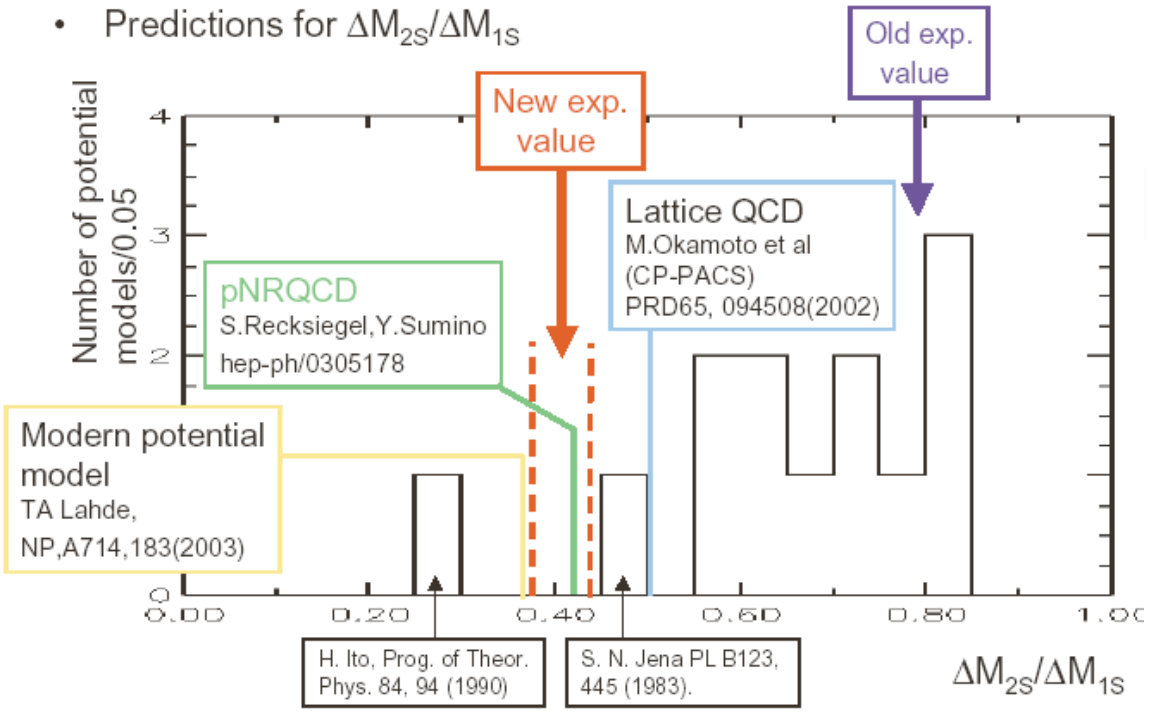

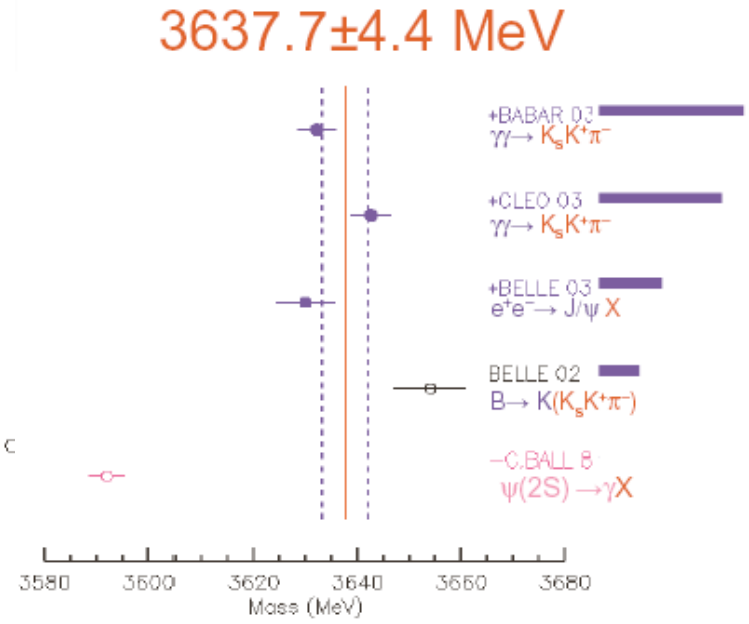

CL=14% scale factor=1.3

New measurements of mass are consistent

Application to quarkonium spectroscopy and determination of α_s, m_b, m_c.

- Global level structure of bottomonium is reproduced. Brambilla, Y.S., Vairo; Recksiegel, Y.S
- Fine and hyperfine splittings of charmonium/bottomonium reproduced.
  Two exceptions in ~2003: Recksiegel, Y.S.; Kniehl, Penin, Pineda, Smirnov, Steinhauser
  charmonium hyperfine splitting $\Psi(2S)$–$\eta_c(2S)$
  bottomonium hyperfine splitting $\Upsilon(1S)$–$\eta_b(1S)$
  Solved in favor of pert. QCD predictions.
- Determination of bottom and charm quark $\overline{\rm MS}$ masses:

$$\overline{m}_b(\overline{m}_b) = 4190 \pm 30 \text{ MeV}$$
$$\overline{m}_c(\overline{m}_c) = 1243 \pm 100 \text{ MeV}$$

Brambilla, Y.S., Vairo

- Relation between lattice α_s and $\overline{\rm MS}$ α_s being accurately measured
  (realistic precision determination in near future) Y.S.
  Brambilla, Petreczky, Tormo, Soto, Vairo

Motivation for precision determinations of heavy quark masses

- Bottom quark
  - Constraints on $b-\tau$ mass ratio of SU(5) GUT models
  - Input param. for *b* physics: e.g. $\Gamma_b \propto m_b^5$ ⇨ LHC$_b$, Super-*B* factory

- Top quark
  - The only quark mass with undefined mass in current PDG data.

$$m_t = 173.21 \pm 0.51 \pm 0.71 \text{ GeV}$$ ⟵ What mass?

$$m_t^{\overline{\text{MS}}} = 160\,^{+5}_{-4} \text{ GeV}$$

- Tests of Yukawa coupling at LHC and beyond.

$$\delta_t M_H^{\text{SM}} \propto m_t^2$$

$$\delta_t M_H^{\text{MSSM}} \propto m_t^4$$

cf. $\Delta M_H \sim 0.1\text{–}0.2 \text{ GeV}$ LHC

$\sim 0.05 \text{ GeV}$ ILC

Particle Data Group 2014

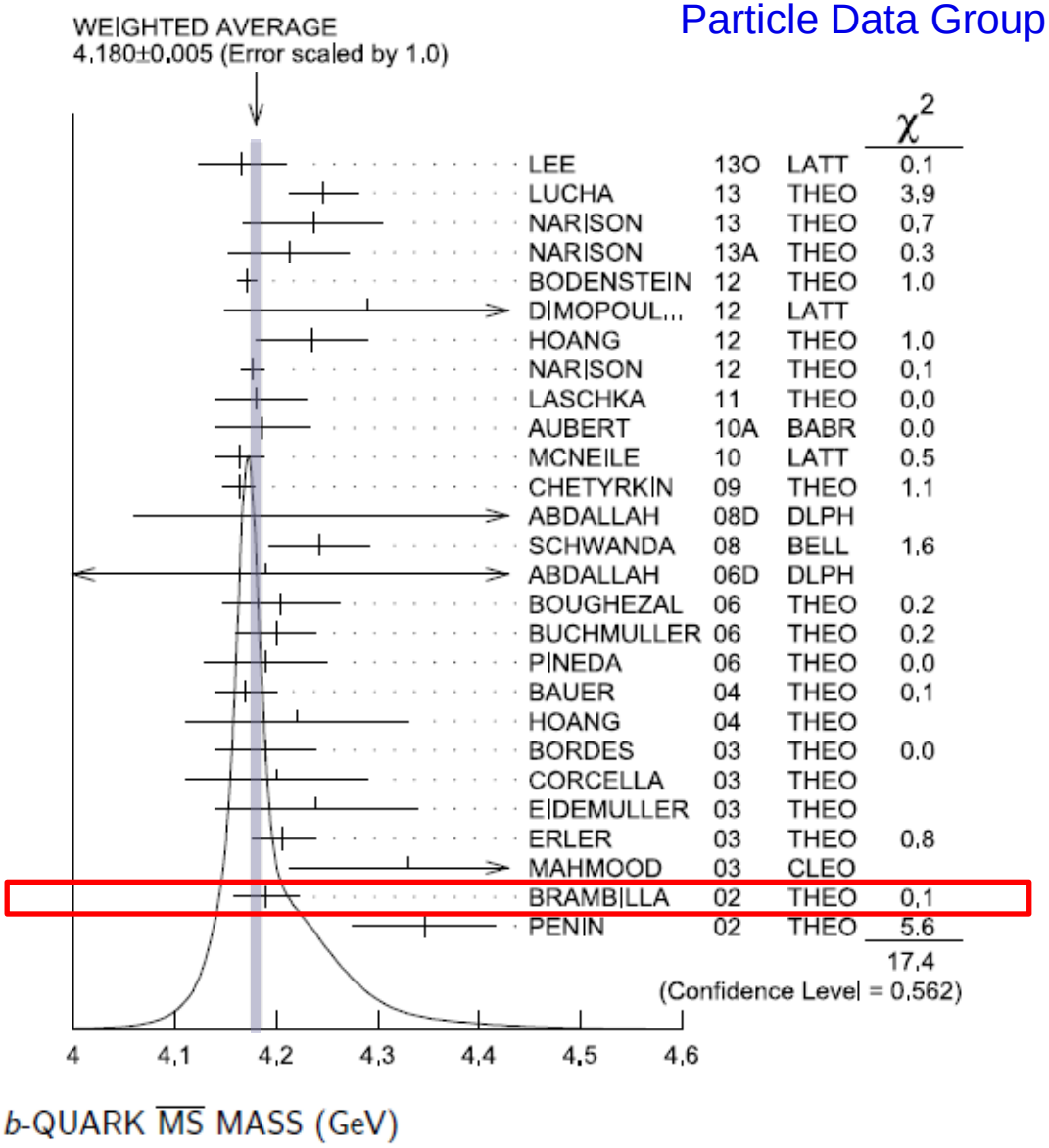

Prospects for precision determination of m_t from $M_{tt}(1S)$

Hoang, et al.

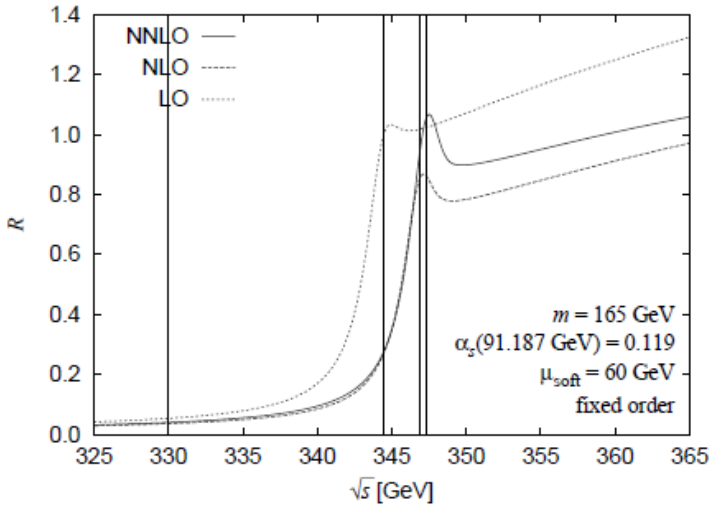

$e^+e^- \to t\bar{t}$ in the threshold region
@ future Linear Collider

$\Delta \overline{m}_t \lesssim 100$ MeV

Hagiwara, Y.S., Yokoya
Kiyo, et al.

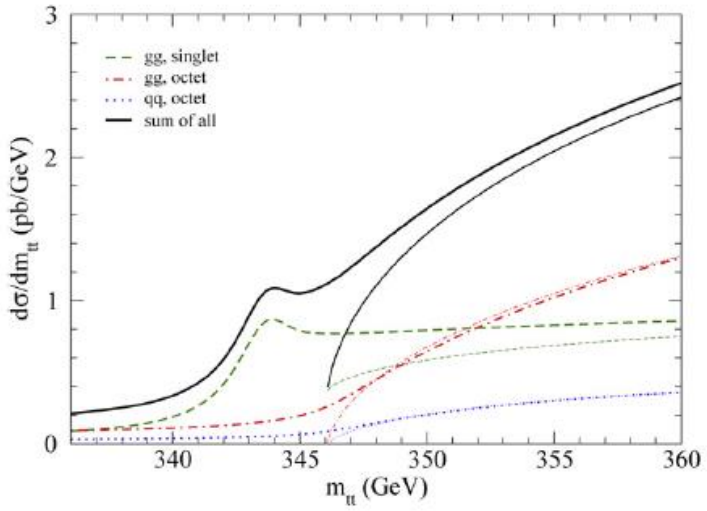

$pp \to t\bar{t}$ (threshold region)
@LHC

$\Delta \overline{m}_t$ significantly smaller than 1GeV?

Application to quarkonium spectroscopy and determination of α_s, m_b, m_c.

- Global level structure of bottomonium is reproduced. Brambilla, Y.S., Vairo
  Recksiegel, Y.S
- Fine and hyperfine splittings of charmonium/bottomonium reproduced.
  Two exceptions in ~2003: Recksiegel, Y.S.; Kniehl, Penin,
  charmonium hyperfine splitting $\Psi(2S)$–$\eta_c(2S)$ Pineda, Smirnov, Steinhauser
  bottomonium hyperfine splitting $\Upsilon(1S)$–$\eta_b(1S)$
  Solved in favor of pert. QCD predictions.
- Determination of bottom and charm quark $\overline{\text{MS}}$ masses:

$$\overline{m}_b(\overline{m}_b) = 4190 \pm 30 \text{ MeV}$$
$$\overline{m}_c(\overline{m}_c) = 1243 \pm 100 \text{ MeV}$$

Brambilla, Y.S., Vairo

⇨ • Relation between lattice α_s and $\overline{\text{MS}}$ α_s being accurately measured
(realistic precision determination in near future) Y.S.
Brambilla, Petreczky, Tormo, Soto, Vairo

Numerical evaluation of action density

3D plot of $\sqrt{\rho_{\beta_0}(\vec{x},\vec{r})} \propto \left|\vec{E}_Q + \vec{E}_{\bar{Q}}\right|$ up to $\mathcal{O}(\alpha_S^{10})$

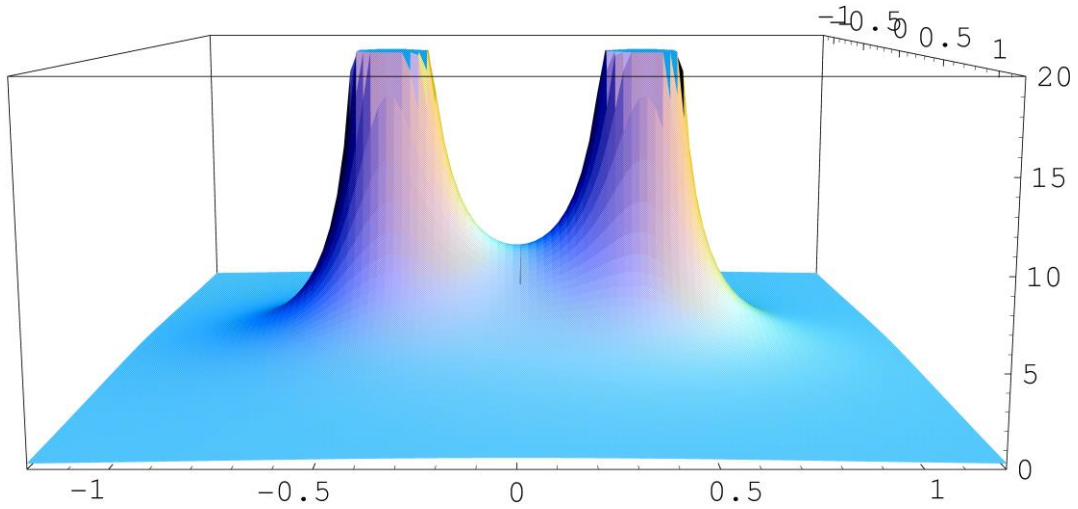

$R = 0.8\ \tilde{\Lambda}^{-1} \approx 0.4$ fm

☆Energy density surrounding heavy quarks

At $R \lesssim \Lambda_{\rm QCD}^{-1}$

- $\rho_{\beta_0}(\vec{x},\vec{r}) \propto \left[\vec{E}_Q(\vec{x}) + \vec{E}_{\bar{Q}}(\vec{x})\right]^2$

  action density $\approx$ energy density in the large-β_0 approx.

- Color electric field ($\propto\sqrt{\rho(\vec{x},\vec{r})}$) between Q and $\bar{Q}$ is stronger than pure Coulomb field $\Longleftarrow$ $\nabla V_L(R)$

- Domain of color electric field (action density) grows isotropically and scales as $\sim R^3$

- Action density distributions corresponding to "Coulomb" and linear potentials:

$$\int d^3\,\vec{x}\ \textit{"Coulomb"} \times \textit{"Coulomb"} \Longrightarrow \textit{"Coulomb"}$$

$$\int d^3\,\vec{x}\ \textit{"Coulomb"} \times \textit{linear} \Longrightarrow \textit{linear}$$

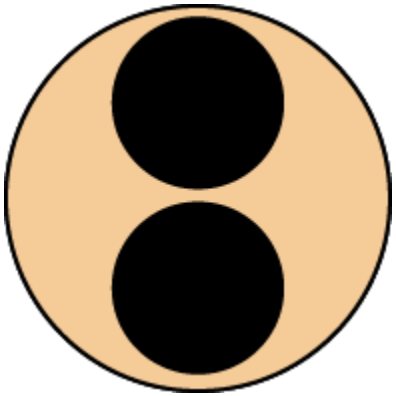

Casimir scaling hypothesis

····· supported by lattice measurements

Markum,Faber
Campbell,Jorysz,Michael
Deldar
Bali

$$V_R(r) \propto C_R$$

2nd Casimir op. for rep. R

cf. $V_R^{\rm tree}(r) = -C_R \dfrac{\alpha_s}{r}$

2-loop

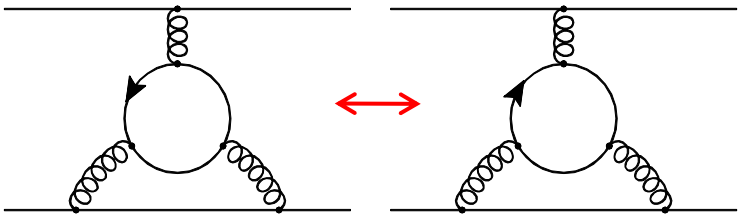

$$\left(d_R^{a_1,\cdots a_n} = \frac{1}{n!} \mathrm{Tr}\left[T_R^{a_1} T_R^{a_2} \cdots T_R^{a_n} + (\text{all permutations}) \right] \right)$$

$d_R^{abc} d_F^{abc}$ cancel

$d_A^{abc} = 0$ by $(T_A^a)^T = -T_A^a$

protected by C-inv.

3-loop

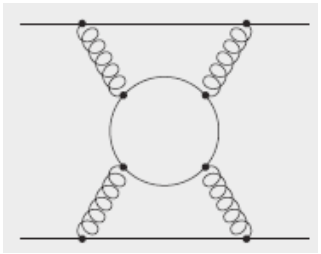

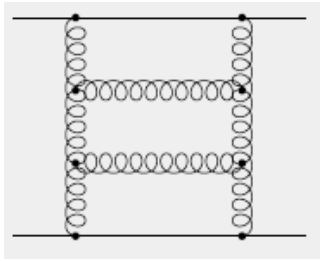

$d_R^{abcd} d_F^{abcd}$ $d_R^{abcd} d_A^{abcd}$

Anzai, Kiyo, YS

⇨ Casimir scaling violation

Tiny violation predicted, compatible with current lattice data.

☆Summary

1. Before 1998: Theoretical problem

   IR ambiguity (renomalon)

2. Around 1998: Drastic improvement

   Discovery of cancellation of renormalons

   Interpretation, a linear potential at $r \lesssim \Lambda_{\rm QCD}^{-1}$

3. After 1998: Applications

   Spectroscopy

   Decays

   Determinations of m_b, m_c (m_t)

   Determination of α_s

   Gluon config. inside quarkonium

   Casimir scaling violation for static potential

   ⋮

☆Summary

Which extent is predictive power of perturbative QCD?

- OPE of $V_{\mathrm{QCD}}(r)$
- Log resummation in $V_{UV}(r;\mu_f)$

Short-distance expansion

combines with non-pert. matrix element

$$\boldsymbol{V_{\mathrm{QCD}}(r) \sim \frac{c_{-1}}{r} + c_0 + c_1 r + c_2 r^2 + \cdots} \quad \text{at } \boldsymbol{r \ll \Lambda_{\mathrm{QCD}}^{-1}}$$

Genuinely UV contr. $V_C(r) + \sigma r$ identified in pert. prediction.

Generalization to other observables?

Renormalon in the QCD potential

Aglietti, Ligeti

$$\alpha_{1L}(q) = \frac{\alpha_S(\mu)}{1+\frac{\beta_0\alpha_S(\mu)}{4\pi}\log\left(\frac{q^2}{\mu^2}\right)} = \frac{4\pi/\beta_0}{\log\left(\frac{q^2}{\Lambda^2}\right)}$$

$$\Lambda \equiv \mu\,\exp\left[-\frac{2\pi}{\beta_0\alpha_S(\mu)}\right]$$

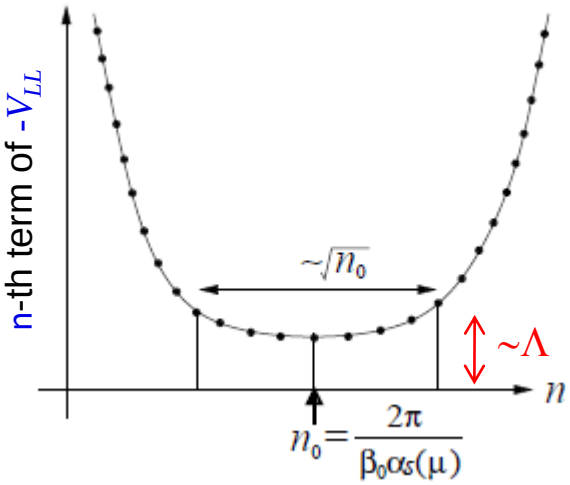

$$V_{LL}(r) = -\int\frac{d^3\vec{q}}{(2\pi)^3}\,e^{i\vec{q}\cdot\vec{r}}\,C_F\,\frac{4\pi\alpha_{1L}(q)}{q^2}$$

ill defined

$$= -C_F\,4\pi\alpha_S(\mu)\sum_{n=0}^{\infty}\int\frac{d^3\vec{q}}{(2\pi)^3}\,\frac{e^{i\vec{q}\cdot\vec{r}}}{q^2}\left\{-\frac{\beta_0\alpha_S(\mu)}{4\pi}\log\left(\frac{q^2}{\mu^2}\right)\right\}^n$$

$$= -C_F\,4\pi\alpha_S(\mu)\sum_{n=0}^{\infty}\left\{\frac{\beta_0\alpha_S(\mu)}{4\pi}\right\}^n f_n(r,\mu)\times n!$$

$$F(r,\mu;u) \equiv \int\frac{d^3\vec{q}}{(2\pi)^3}\,\frac{e^{i\vec{q}\cdot\vec{r}}}{q^2}\left(\frac{\mu^2}{q^2}\right)^u = \frac{(\mu r/2)^{2u}}{4\pi^{3/2}r}\,\frac{\Gamma(\frac{1}{2}-u)}{\Gamma(1+u)}$$

$$= \int\frac{d^3\vec{q}}{(2\pi)^3}\,\frac{e^{i\vec{q}\cdot\vec{r}}}{q^2}\exp\left[-u\log\left(\frac{q^2}{\mu^2}\right)\right] = \sum_n f_n(r,\mu)\,u^n$$

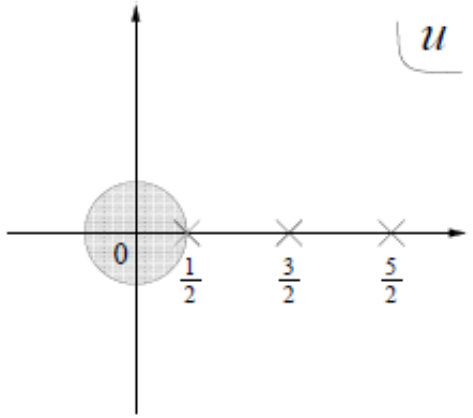

Asymptotically $f_n(r,\mu) \sim \underbrace{\frac{1}{2\pi^2}}_{\| \; -2\,\mathrm{Res}\left[F;u=\frac{1}{2}\right]}\mu\times 2^n$

Most dominant part is indep. of r !

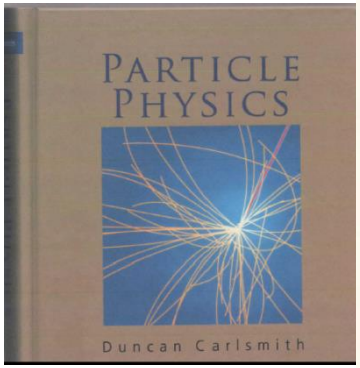

9.4 ■ APPLICATIONS OF HIGH ORDER CALCULATIONS

The computation of radiative corrections entails evaluation of the amplitudes associated with many Feynman diagrams. Such computations are highly technical and require the use of computer programs which can perform symbolic manipulations and reductions to core integrals. By way of illustration, Figure 9.13 shows the result of an analytic calculation including terms of order α_s^4 of the static potential

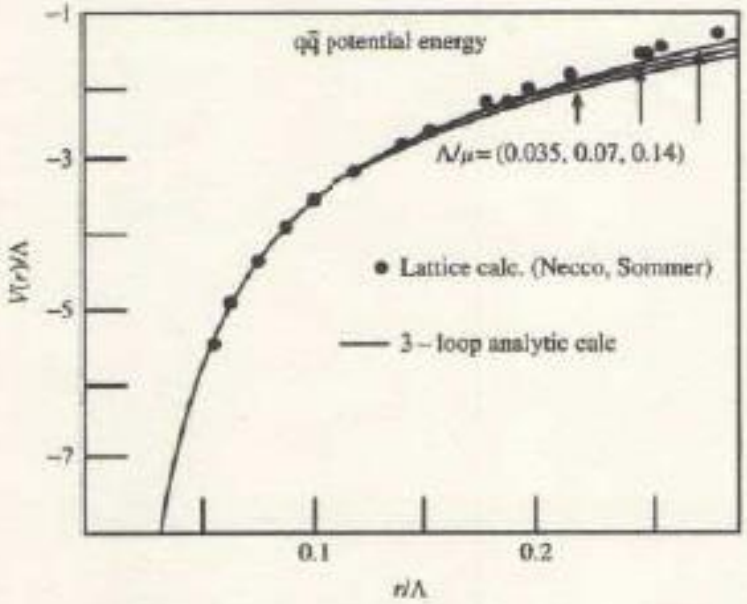

FIGURE 9.13 Computed static color interaction potential at three-loop order compared with the lattice computations. The curves correspond to several choices of renormalization scale. The points represent the results of independent lattice QCD calculations. [C. Anzai, Y. Kiyo, and Y. Sumino, Phys. Rev. Lett. **104**, 112003 (2010)]

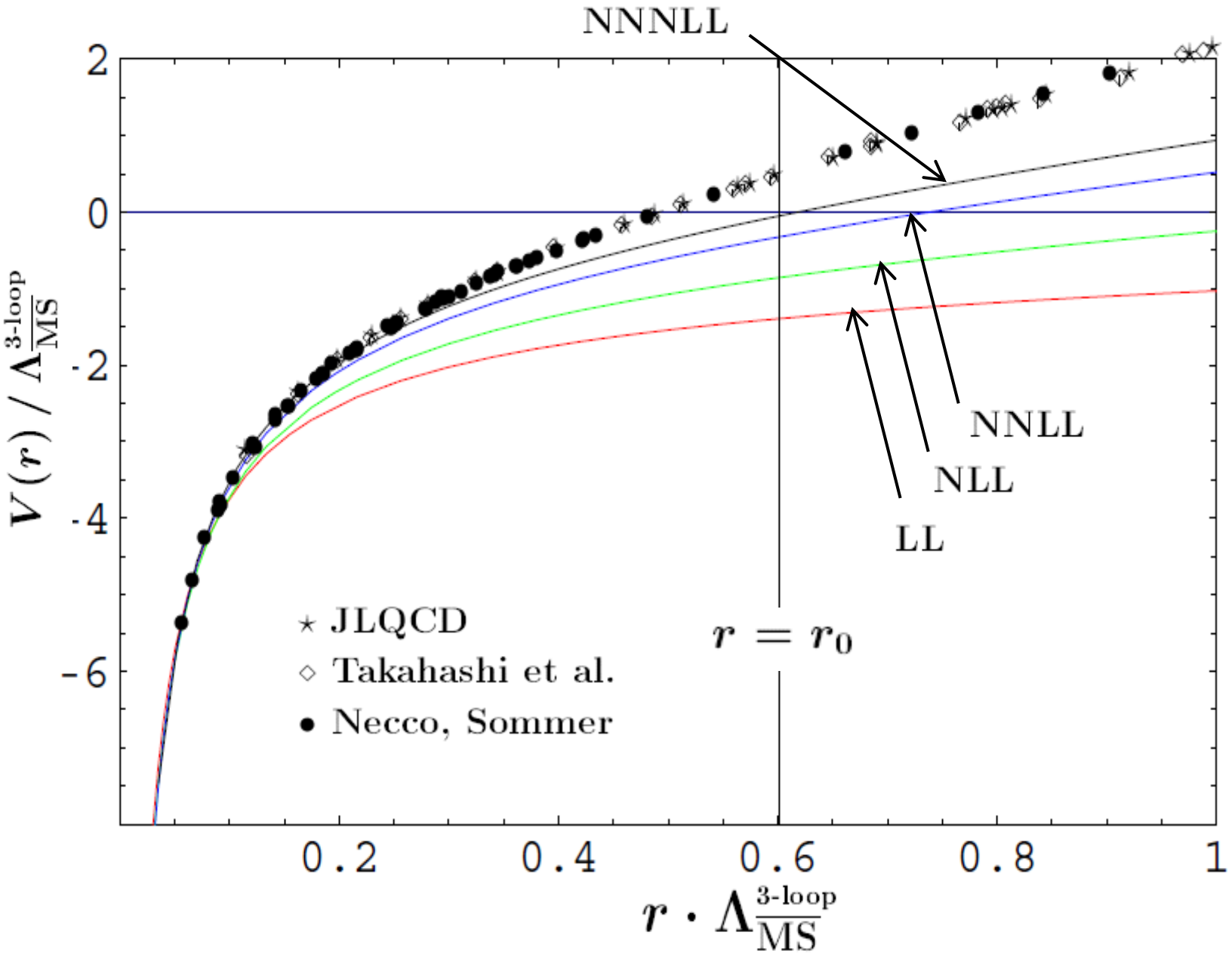
NNNLL
NNLL
NLL
LL
$r = r_0$
⋆ JLQCD
◇ Takahashi et al.
• Necco, Sommer
$V(r) / \Lambda_{\overline{\rm MS}}^{\rm 3\text{-}loop}$
$r \cdot \Lambda_{\overline{\rm MS}}^{\rm 3\text{-}loop}$
2
0
-2
-4
-6
0.2
0.4
0.6
0.8
1

Interquark force

$$F(r) \equiv -\frac{d}{dr}V_{\rm QCD}(r) \equiv -C_F\frac{\alpha_F(1/r)}{r^2}.$$

Renormalization-group equation: $\mu^2\frac{d}{d\mu^2}\alpha_F(\mu) = \beta_F(\alpha_F)$

$\Longrightarrow$ Due to the running of $\alpha_F(1/r)$, the attractive force $|F(r)|$ increases at large r.

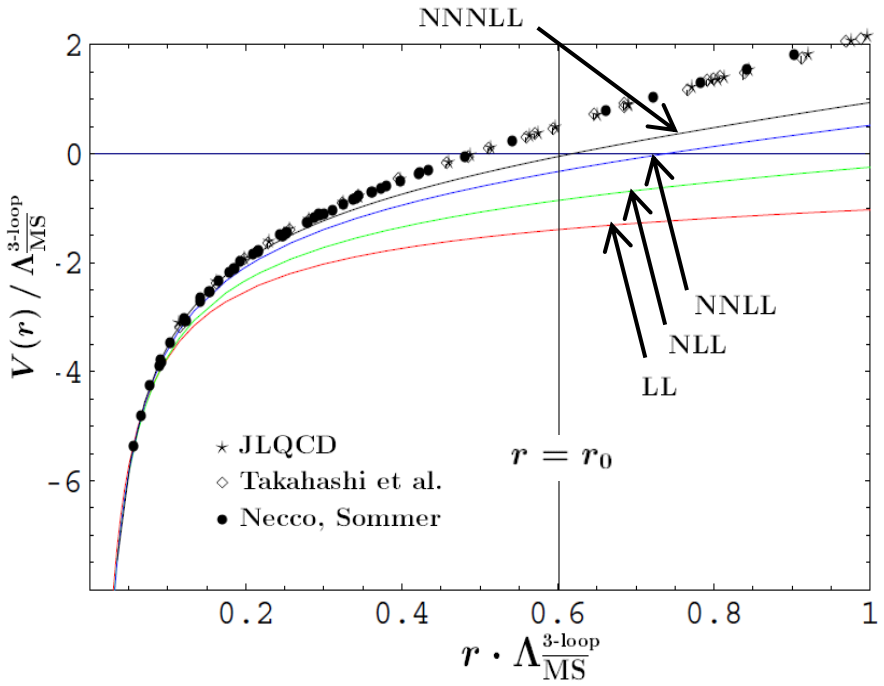

Bottomonium spectrum up to $n = 3$ states

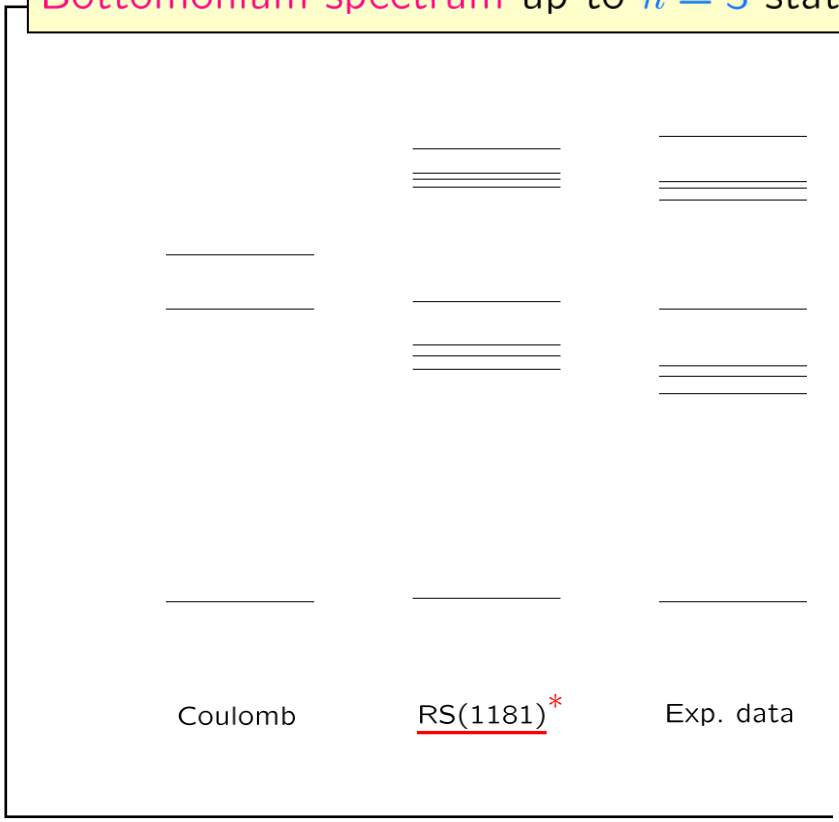

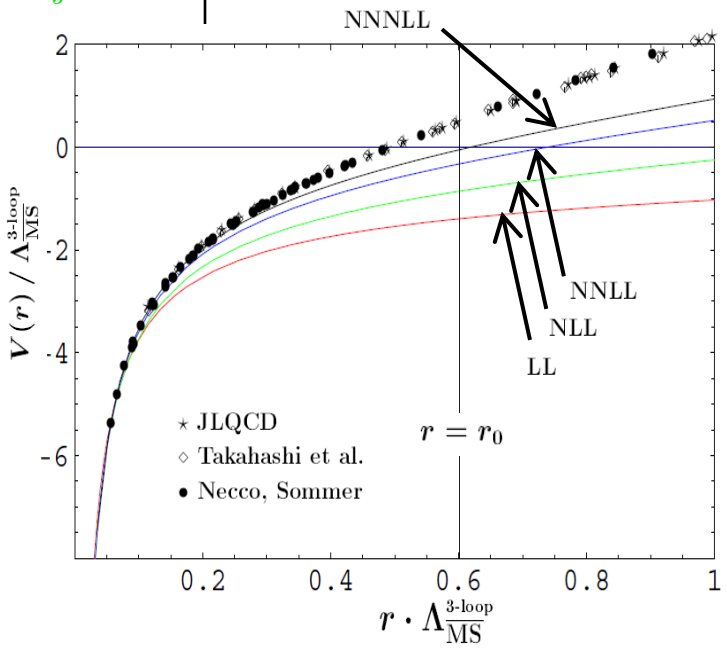

* Pert. QCD prediction including full $\mathcal{O}(\alpha_S^4 m)$ corrections to individual energy levels, as well as full $\mathcal{O}(\alpha_S^5 m)$ corrections to fine structure [$\alpha_S(M_Z) = 0.1181$]. Recksiegel, Y.S.

$$V_{\rm QCD}(r) = \underbrace{V_{\rm pert}(r;\mu_f)}_{\text{Wilson coeff.}} + \underbrace{\delta E(r;\mu_f)}_{\text{non-pert. contr.}}$$

$\delta E \to 0$ as $r \to 0$ $\quad \sim \langle G^a_{\mu\nu}(0)^2 \rangle\, r^3$

Comparison of lattice $V_{\rm QCD}(r)$ and $V_{\rm pert.}(r;\mu_f)$ at short distances

$$V_{\rm latt}(r) - V_{\rm pert}(r;\mu_f) = \delta E(r;\mu_f)$$

$\frac{1}{r\log r}$ $\longleftrightarrow$ cancel $\frac{1}{r\log r}$ $\qquad$ r^3

Sensitive to relation between r_0 and $\Lambda_{\overline{MS}}$ or $\alpha_S(M_Z)$

$r_0 \Lambda^{\text{3-loop}}_{\overline{\rm MS}} = 0.574 \pm 0.042$ Y.S.

c.f. Schrödinger functional method:

0.602 ± 0.048

Capitani, Lüscher, Sommer, Wittig

0.586 ± 0.048

Necco, Sommer

Including 3-loop QCD pot.

$$r_0 \Lambda^{\rm 3-loop}_{\overline{\rm MS}} = 0.622^{+0.019}_{-0.015}$$

Brambilla,Tomo,Soto,Vairo

$$E_X \approx 2m_b^{\overline{MS}}(\mu) + \int_0^{\mu} dq\, f_X(q)\alpha_s(q)$$

Brambilla,YS,Vairo
Recksiegel,YS

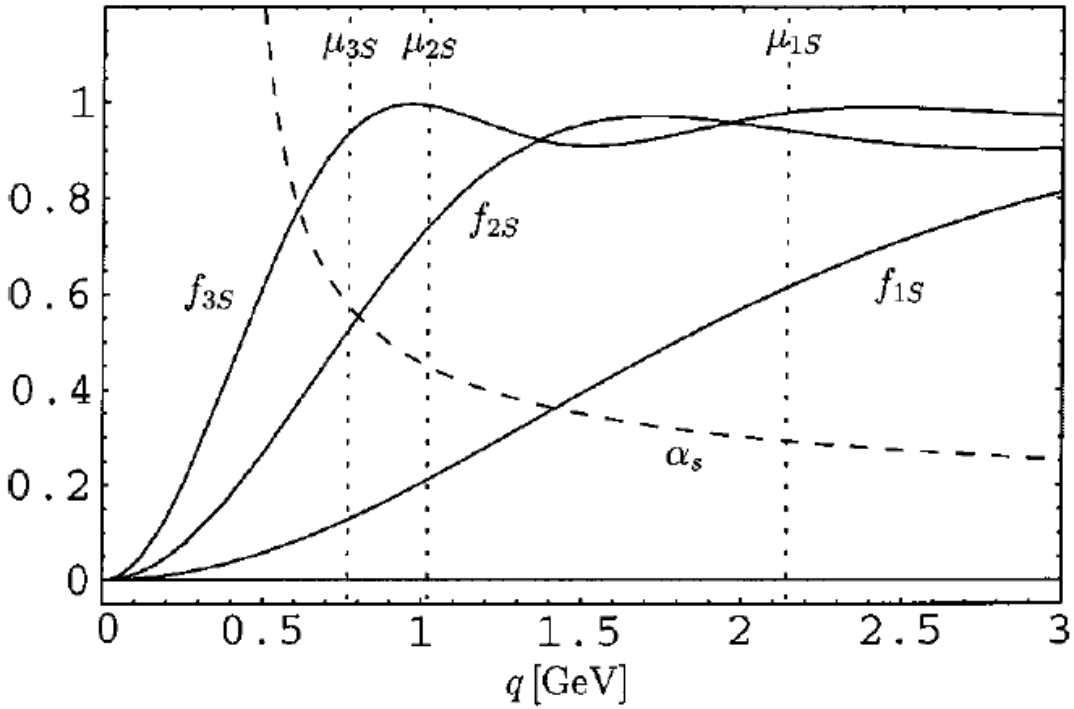

FIG. 5. Support functions for the S states. The solid curves show the support functions as defined in Eq. (19); for comparison of the relevant scales, $\alpha_s^{(4)}(\mu)$ is also plotted (dashed curve). Since the analysis that we advocate in this work does not attribute scales to the individual states, the scales indicated by the dotted lines are taken from [3], Table II.

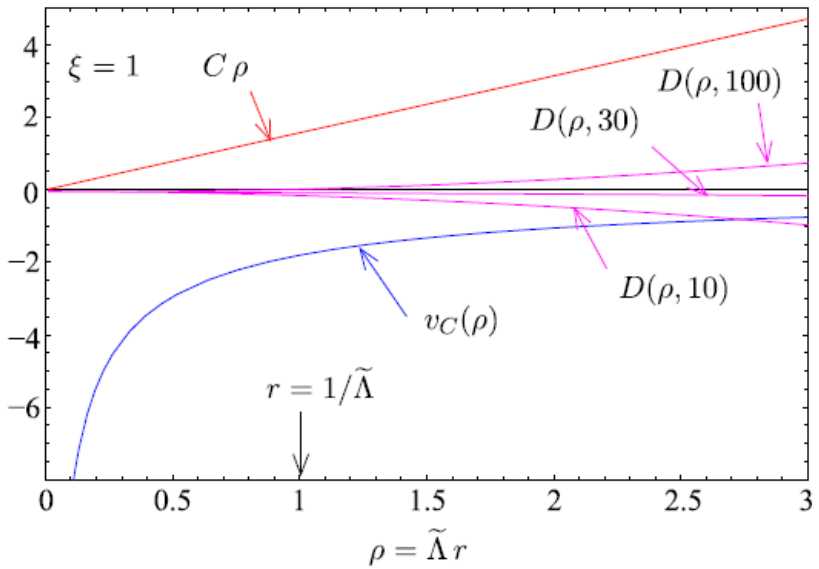

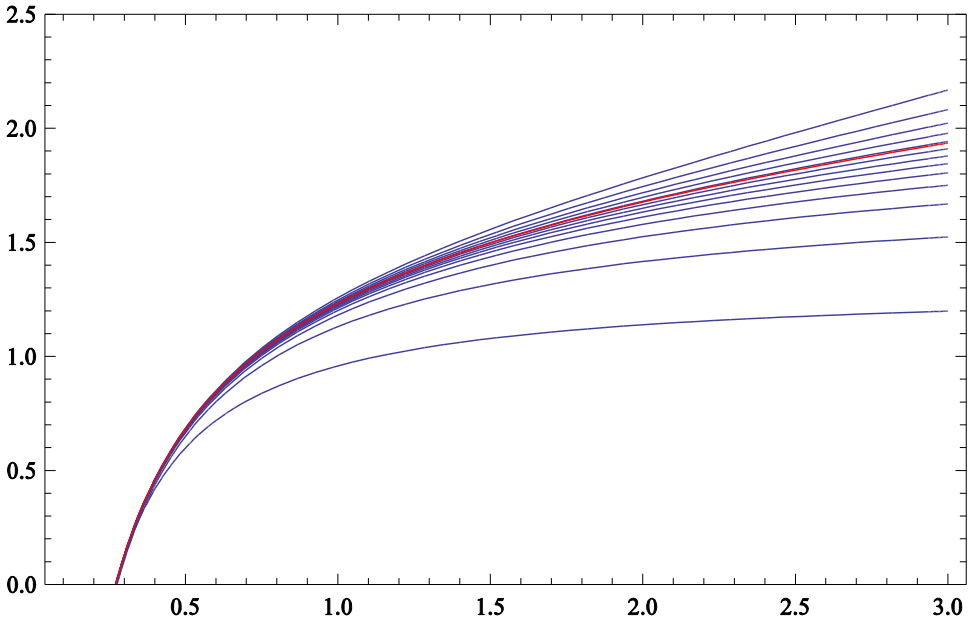

$$V_{\rm UV}(r;\mu_f) \equiv \int_{|q|>\mu_f} \frac{d^3q}{(2\pi)^3}\left[-4\pi C_F \frac{\alpha_V(q)}{q^2}\right]$$

$$V_{\rm UV}(r;\mu_f) - \Big[V_C(r) + \sigma r\Big] = \text{const.} + \mathcal{O}(\mu_f^3 r^2)$$

for $r^{-1} \gg \mu_f \gg \Lambda.$

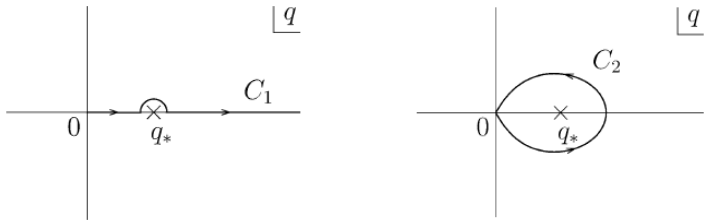

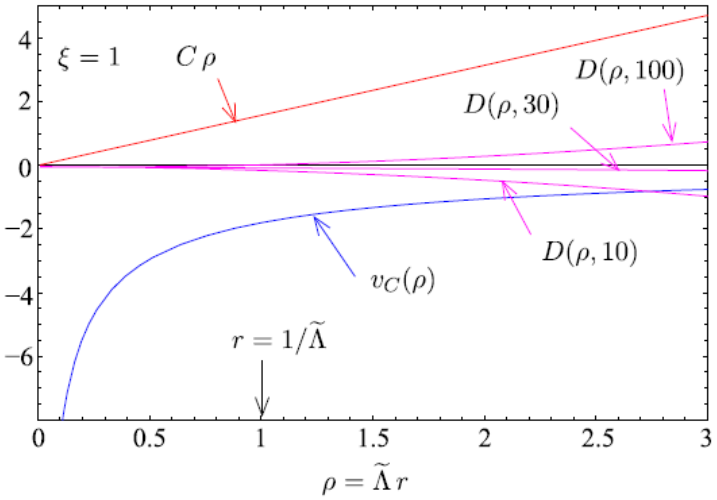

A 'Coulomb+Linear potential' is obtained by resummation of logs: YS

$$V_{\rm QCD}(r) = V_C(r) + \sigma r + \text{const.} + \mathcal{O}(\Lambda^3 r^2)$$

- $$V_C(r) = -\frac{4\pi C_F}{\beta_0 r} - \frac{2C_F}{\pi}\,\mathrm{Im}\int_{C_1} dq\,\frac{e^{iqr}}{qr}\,\alpha_V(q)$$ ← Coulombic pot. with log corr. at short-dist.

$$= \begin{cases} -\frac{2\pi C_F}{\beta_0}\,\frac{1}{r|\log(\Lambda_{\overline{\rm MS}} r)|}\left[1 - \frac{\delta}{2}\,\frac{\log|\log(\Lambda_{\overline{\rm MS}} r)|}{|\log(\Lambda_{\overline{\rm MS}} r)|}\right], & r \to 0, \\ -\frac{4\pi C_F}{\beta_0 r}, & r \to \infty, \end{cases}$$

- $$\sigma = \frac{C_F}{2\pi i}\int_{C_2} dq\, q\,\alpha_V(q)$$ ← Coefficient of linear pot.

$$\alpha_V(q) = \alpha_s(q)\sum_{n=0}^{N} a_n \left(\frac{\alpha_s(q)}{4\pi}\right)^n$$

$N = 0, 1, 2, 3, \cdots$ for LL, NLL, NNLL, NNNLL, $\cdots$.

e.g. $$\sigma_{\rm NLL} = \frac{2\pi C_F}{\beta_0}\left(\Lambda^{\text{2-loop}}_{\overline{\rm MS}}\right)^2 \frac{e^{-\delta}}{\Gamma(1+\delta)}\left[1 + \frac{a_1}{\beta_0}\,\delta^{-1-\delta}\,e^{\delta}\,\gamma(1+\delta,\delta)\right]$$

$\delta = \beta_1/\beta_0^2$

μ dependence and convergence of $M_{tt}(1S)$

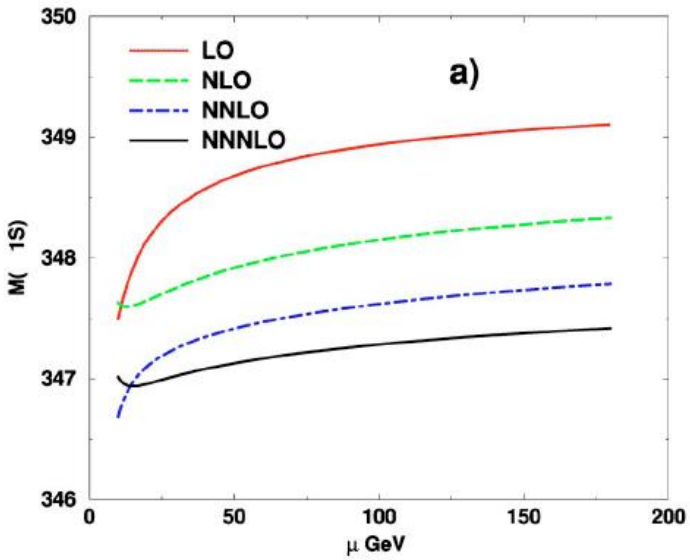

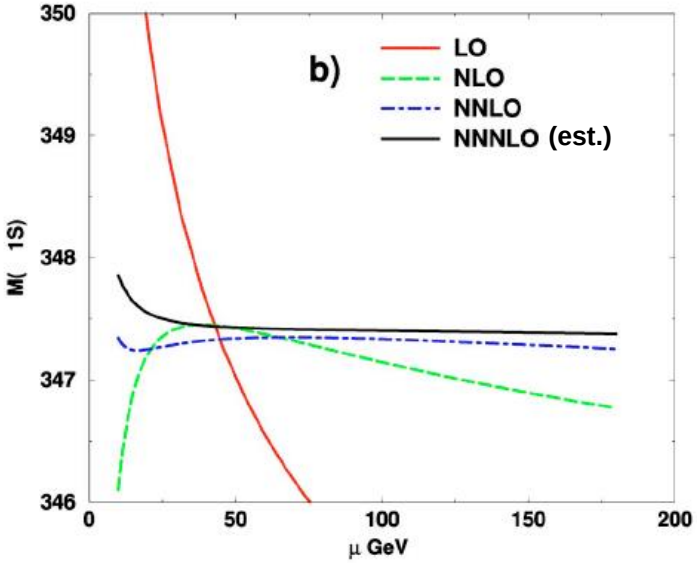

- $\Upsilon(1S)$: $M_{\Upsilon(1S)} = \mathbf{9.94 - 0.10 - 0.15 - 0.20 - 0.26}$ GeV (Pole-mass scheme)
  $= \mathbf{8.43 + 0.65 + 0.26 + 0.10 + 0.01}$ GeV ($\overline{\text{MS}}$ scheme)
- $\Upsilon(2S)$: $M_{\Upsilon(2S)} = \mathbf{9.94 - 0.06 - 0.11 - 0.22 - 0.41}$ GeV (Pole-mass scheme)
  $= \mathbf{8.43 + 1.07 + 0.30 + 0.13 + 0.01}$ GeV ($\overline{\text{MS}}$ scheme)